AD-A078 036 VARIAN ASSOCIATES INC PALO ALTO CA F/G 9/5
MULTIBAND KLYSTRON STUDY.(U)
OCT 79 A D LARUE F30602-78-C-0124
UNCLASSIFIED RADC -TR-79-248 NL

1 OF 1
AD A078036

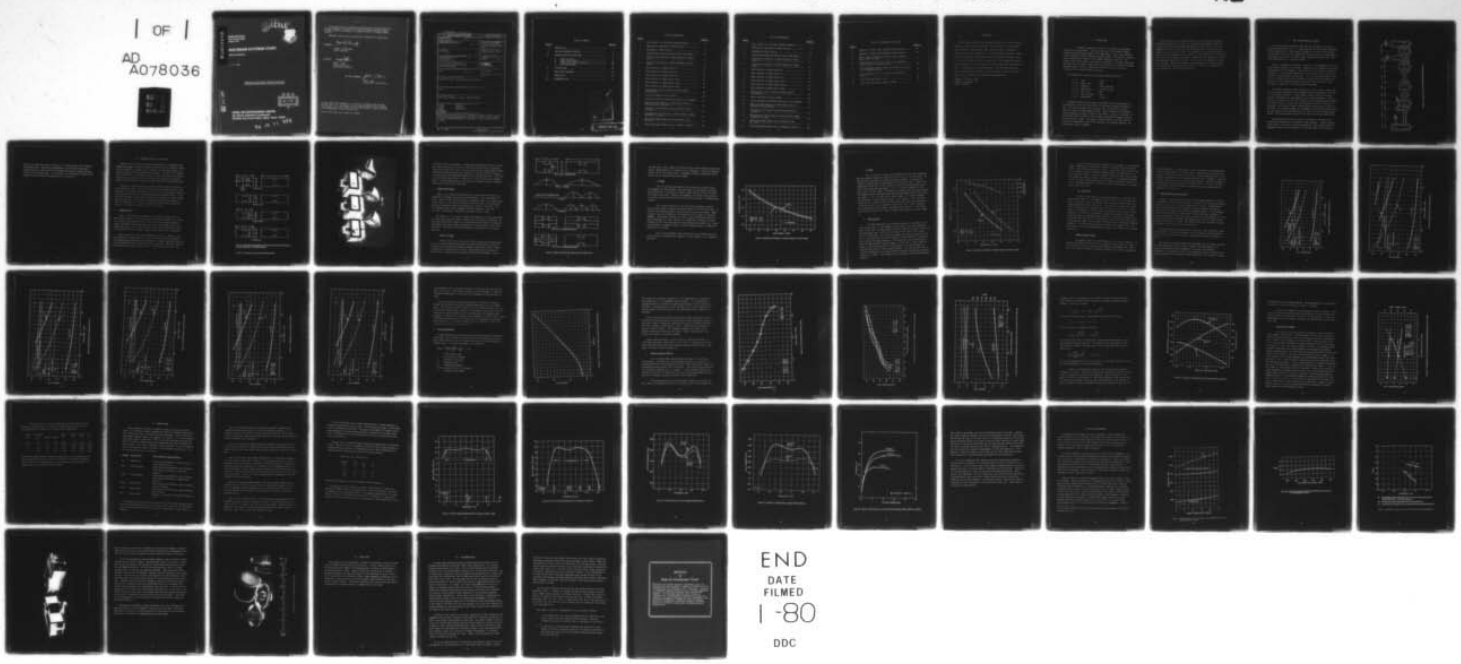

END
DATE FILMED
1-80
DDC

LEVEL II

RADC-TR-79-248
Final Technical Report
October 1979

MULTIBAND KLYSTRON STUDY

Varian Associates

A. D. LaRUE

ROME AIR DEVELOPMENT CENTER
Air Force Systems Command
Griffiss Air Force Base, New York 13441

This report has been reviewed by the RADC Public Affairs Office (PA) and is releasable to the National Technical Information Service (NTIS). At NTIS it will be releasable to the general public, including foreign nations.

RADC-TR-79-248 has been reviewed and is approved for publication.

APPROVED: Joseph J. Polniaszek

JOSEPH J. POLNIASZEK
Project Engineer

APPROVED: Frank J. Rehm

FRANK J. REHM
Technical Director
Surveillance Division

FOR THE COMMANDER: John P. Huss

JOHN P. HUSS
Acting Chief, Plans Office

If your address has changed or if you wish to be removed from the RADC mailing list, or if the addressee is no longer employed by your organization, please notify RADC (OCTP), Griffiss AFB NY 13441. This will assist us in maintaining a current mailing list.

Do not return this copy. Retain or destroy.

UNCLASSIFIED

SECURITY CLASSIFICATION OF THIS PAGE (When Data Entered)

REPORT DOCUMENTATION PAGE

READ INSTRUCTIONS BEFORE COMPLETING FORM

1. REPORT NUMBER: RADC-TR-79-248	2. GOVT ACCESSION NO.
3. RECIPIENT'S CATALOG NUMBER	
4. TITLE (and Subtitle): MULTIBAND KLYSTRON STUDY	5. TYPE OF REPORT & PERIOD COVERED: Final Technical Report, 31 Mar 78 — 30 Jun 79
6. PERFORMING ORG. REPORT NUMBER: N/A	
7. AUTHOR(s): A. D. LaRUE	8. CONTRACT OR GRANT NUMBER(s): F30602-78-C-0124
9. PERFORMING ORGANIZATION NAME AND ADDRESS: Varian Associates, Inc., 611 Hansen Way, Palo Alto CA 94303	10. PROGRAM ELEMENT, PROJECT, TASK AREA & WORK UNIT NUMBERS: 45061228
11. CONTROLLING OFFICE NAME AND ADDRESS: Rome Air Development Center (OCTP), Griffiss AFB NY 13441	12. REPORT DATE: October 1979
	13. NUMBER OF PAGES: 61
14. MONITORING AGENCY NAME & ADDRESS (if different from Controlling Office): Same	15. SECURITY CLASS. (of this report): UNCLASSIFIED
	15a. DECLASSIFICATION DOWNGRADING SCHEDULE: N/A

16. DISTRIBUTION STATEMENT (of this Report)

Approved for public release; distribution unlimited.

17. DISTRIBUTION STATEMENT (of the abstract entered in Block 20, if different from Report)

Same

18. SUPPLEMENTARY NOTES

RADC Project Engineer: Joseph J. Polniaszek (OCTP)

19. KEY WORDS (Continue on reverse side if necessary and identify by block number)

S-Band	Multiband
C-Band	Klystron
Cavity	Electron Beam
Bandwidth	
Broadband	

20. ABSTRACT (Continue on reverse side if necessary and identify by block number)

The present study indicates that a reasonable interspersed S-Band and C-Band cavity broadband multiband klystron is feasible. Computer results suggest a 10 percent operating bandwidth at S-Band and a 5 percent operating band at C-Band.

DD FORM 1 JAN 73 1473

UNCLASSIFIED

SECURITY CLASSIFICATION OF THIS PAGE (When Data Entered)

364 100

TABLE OF CONTENTS

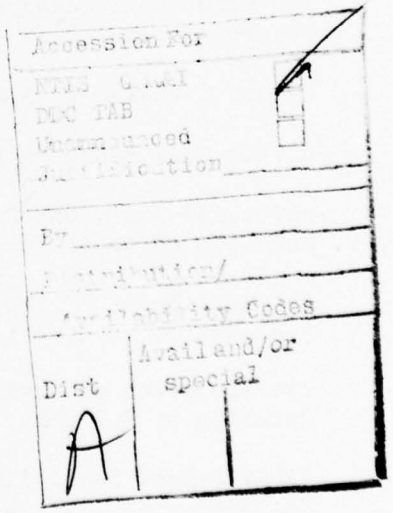

LIST OF ILLUSTRATIONS

LIST OF ILLUSTRATIONS

LIST OF ILLUSTRATIONS (Continued)

EVALUATION

Wide Frequency Diversity has long been recognized as a most effective electronic counter measure technique. However, the cost of acquisition and maintenance of two separate radar systems has been a large determining factor in its application. If the Wide Frequency Diversity concept could be embodied in a single radar system, its tactical advantage could be realized at minimal increase in these costs. This program endeavored to prove feasibility of a key component in such a system, the final amplifier tube. Through the effort expended herein, it has been determined that the multiband klystron concept is sound and presently efforts are being made at the construction of an advanced development model.

Joseph P. Polniaszek

JOSEPH P. POLNIASZEK
Project Engineer

I. INTRODUCTION

Frequency diversity is held to be an effective ploy against electronics countermeasures. The only viable use of wide range frequency diversity with existing equipment is the employment of two or more separate radars operating in widely different frequency bands. This solution, however, may be prohibitive in terms of size, weight, complexity, and cost. The present study effort aims at the ultimate development of a single linear beam microwave device capable of high power pulse operation in two widely separated frequency bands, so that a single radar using the tube will enjoy the advantage of wide range frequency diversity.

The experimental tube has the following parameters as goals:

4.1.5.1	Gain	40 dB
4.1.5.2	Power, Peak	3 MW
4.1.5.3	Bandwidth	10% in each band
4.1.5.4	Band Centers	3.3 and 5.65 GHz
4.1.5.5	Efficiency	40%
4.1.5.6	Power, Average	8 kW
4.1.5.7	Pulse Width	10 μsec

Preliminary efforts in the study of multimode cavities concentrated on the properties of the box cavity main (1-1) mode and the higher frequency 1-3 mode. The latter has been used in klystron test oscillators in the past because of the wide tuning ranges possible. While a klystron could undoubtedly be designed to operate in both of these modes, it would, of necessity, be a narrow-band device because of the relatively low Rsh/Q and modest coupling factor M in the 1-3 mode. The figure of merit $M^2(R/Q)$ for the mode would be very low by comparison to that of the cavities of an alternate approach, the interspersed cavity arrangement.

The multiband klystron approach having the best chances of success as a broadband operating device is felt to be one employing separate S-band and C-band cavity structures interspersed along the electron beam. Such an arrangement allows the cavities for each operating band to be optimized with respect to their individual bands. The designer has considerable latitude in the selection of parameters for optimization of coupling factor M, Rsh/Q, mode distribution, and operating efficiency. Admittedly some compromise in cavity gap-to-gap spacings must be accepted. This is felt to be amenable to study and adjustment. Many different gap-to-gap arrangements in klystron design yield essentially similar operational results. This report concentrates on the interspersed cavity multiband klystron.

II. DUAL MODE BROADBAND KLYSTRON

Dual mode broadband microwave tubes have been designed to operate at widely different power levels. In some instances both pulsed and CW operation have been achieved in a single device, though over the same operating band. In the present study one is concerned with pulse operation at a multimegawatt peak power level but over two rather widely separated frequency bands, centered specifically on 3.3 and on 5.65 GHz.

Figure 1 illustrates the status of a study of the configuration of a dual mode broadband klystron of this type. S-band and C-band resonant cavities are interspersed in the arrangement. Drift tunnel size is dictated by C-band requirements. S-band cavities among C-band cavities must not have modes competing at C-band fundamental frequencies. The illustration gives detail only so far as resonant cavity center-to-center distances and cavity heights are concerned. It is a working drawing to see that S-band and C-band cavity spacings are compatible in the interspersed arrangement.

According to computer results discussed in a later section, S-band resonant cavity spacings should yield reasonable klystron performance over close to a ten percent bandwidth. C-band computer results indicate relatively marginal performance over approximately a five percent bandwidth. Further work will be necessary in the C-band design in any hardware program following the present effort. An additional C-band resonant cavity will probably be necessary. The center-to-center spacing between S-band cavities S-3 and S-4 may have to be increased somewhat to accommodate the additional C-band cavity, and some further S-band adjustments may be required to obtain design optimization. The S-band problem involved in all this is not viewed with concern.

Both S-band and C-band input circuits considered so far make use of coupled-cavity systems in the interest of wide bandwidth. Similar coupled-cavity output circuits have also been considered. These coupled-cavity arrangements have one cavity coupled to the electron beam at the interaction

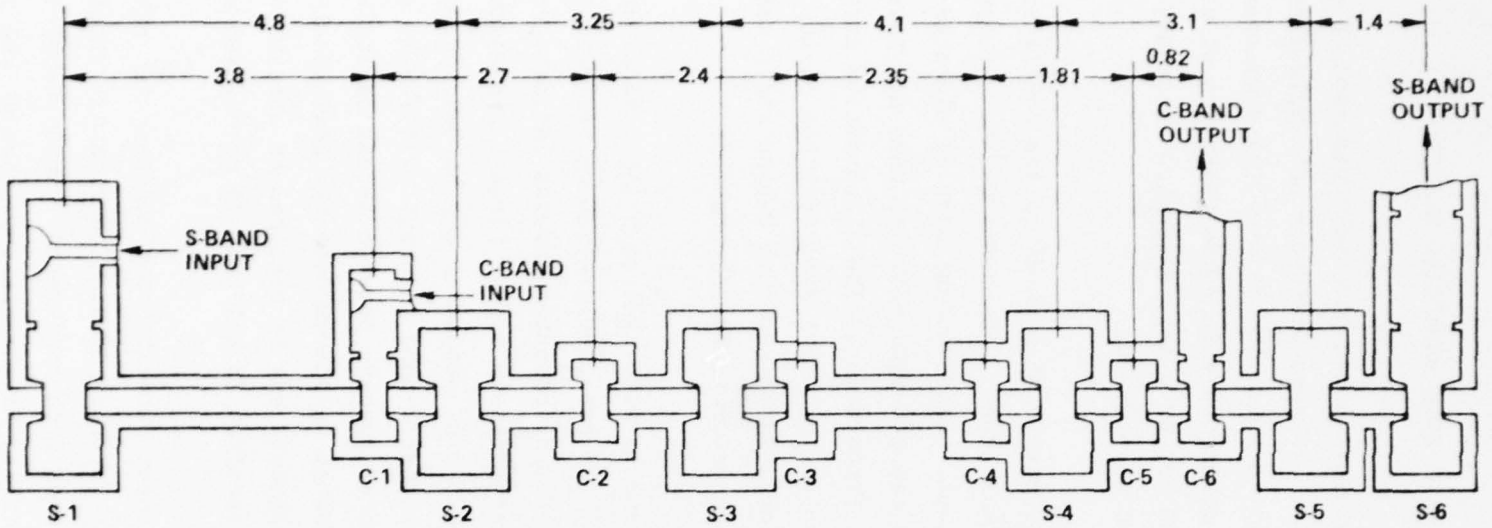

Figure 1. Cavity Layout of a Dual Mode Broadband Klystron

gap, with an additional cavity coupled in as a series filter in the microwave transmission line. There may be advantages in the use of EIK type output system cavities, in which both of the coupled cavities have interaction gaps coupled to the electron beam. It is proposed that consideration be given this possibility before hardware implementation is considered.

III. RESONANT CAVITY COLD TEST WORK

Resonant cavity cold test work had the objectives of determining basic dimensions leading to freedom from mode interference up in frequency through the second harmonic, relative ease of tuning, acceptable Rsh/Q values, and electron beam-to-cavity coupling factors leading to optimum or near optimum values of M^2 (Rsh/Q). Box-shaped resonant cavities were chosen for study because they tune relatively easily and because they provide one additional dimension over cylindrical cavities for shifting possible interfering modes.

Initially it had been planned to perform resonant cavity cold tests at both S-band and C-band. S-band was deemed the more important because it was necessary to avoid mode interference not only in the second harmonic region in these cavities, but also in the intervening C-band frequency region. It was also felt that much of the S-band work would be applicable to C-band through scaling techniques. In any event, C-band work was deferred repeatedly in favor of other efforts. It will be necessary to perform some C-band cold tests before hardware implementation can be considered.

A. S-BAND CAVITIES

Figure 2 illustrates the dimensions of experimental S-band cavities. Drift tunnel diameter (0.375") was dictated by C-band considerations. Most of the testing was accomplished with 0.500 inch drift tube interaction gaps, though considerable study went into cavity S-2A, which employed three different gap sizes, 0.500, 0.550, and 0.600 inches. Drift tube tips allowed a 0.015 inch wide flat all around, a dimension not shown in the illustration.

Figure 3 shows the first three experimental cavities. Cavity S-2 was later modified to become cavity S-2A, and a new cavity S-1A was assembled. The sampling probes shown were later changed to eliminate responses associated with the measuring system, rather than with the cavities. The final sampling probe design used loops of about 1/16th x 1/16th inch cross section. The

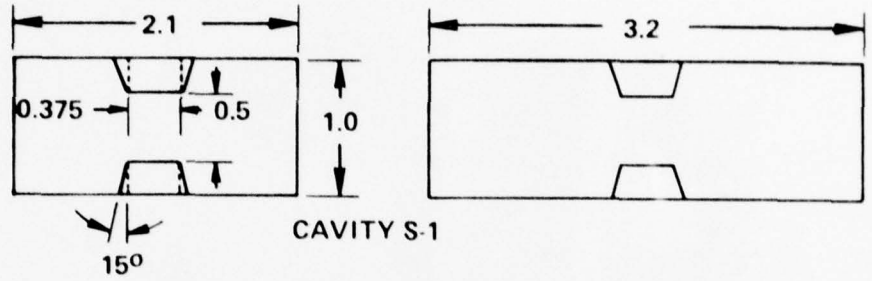

CAVITY S-1

CAVITY S-1A

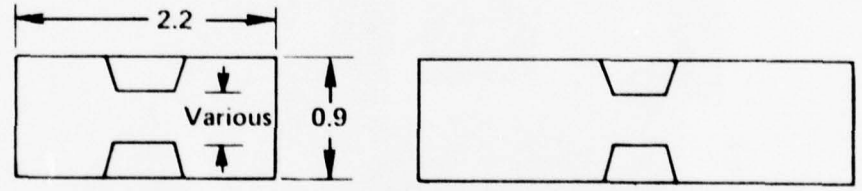

CAVITY S-2A

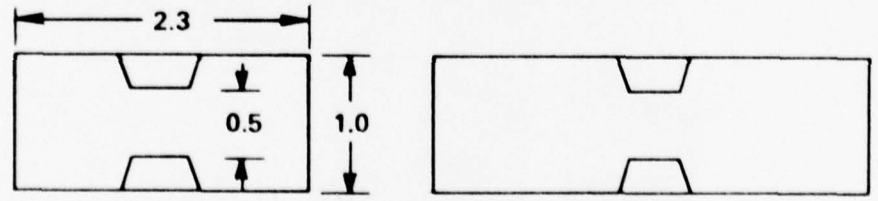

CAVITY S-3

CAVITY LENGTHS (3.2 INCHES) ARE INITIAL LENGTHS, SHORTENED IN STEPS DURING TEST PROCEDURES.

Figure 2. Dimensions of Experimental S-Band Cavities

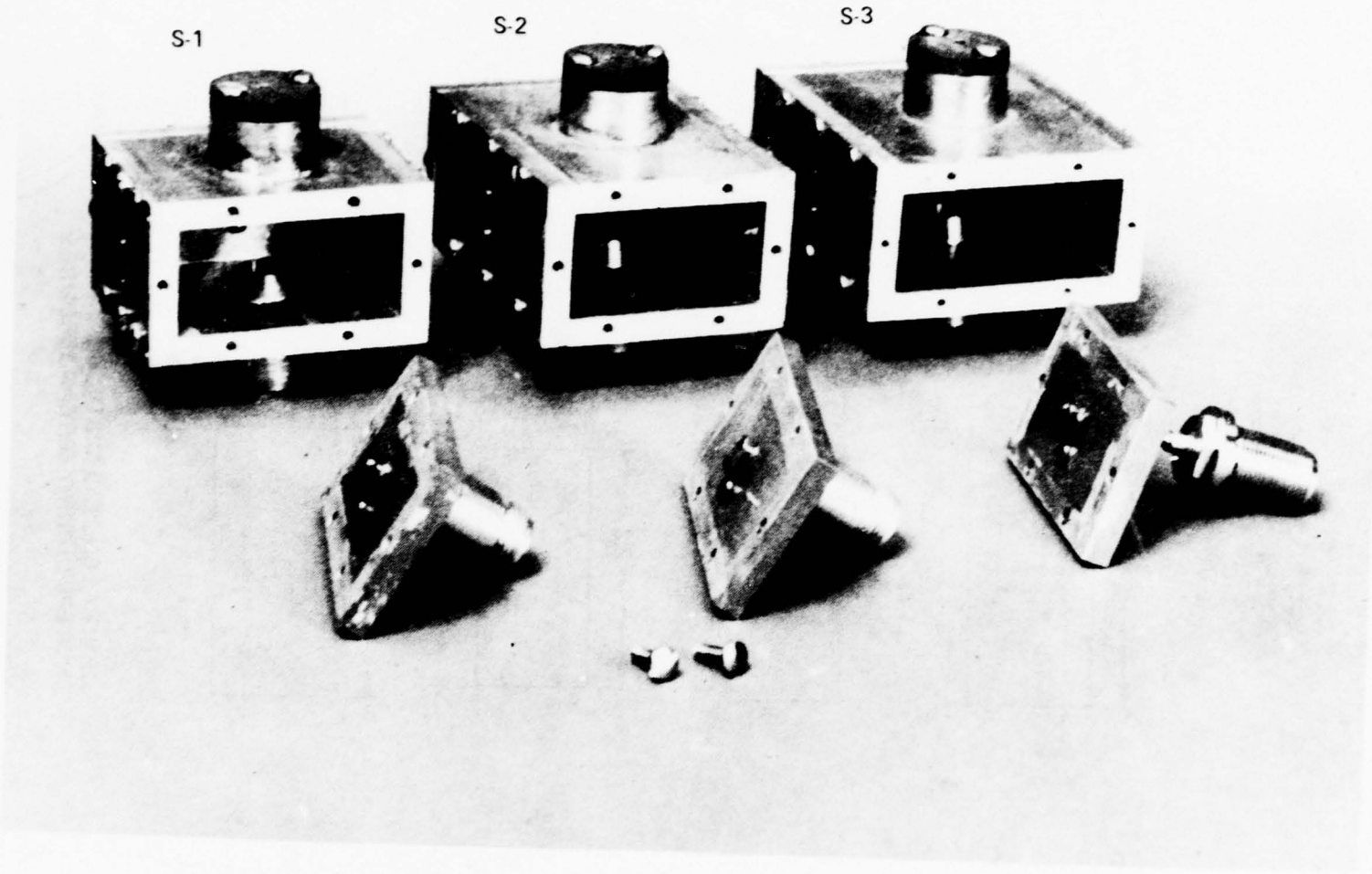

Figure 3. Experimental S-Band Cavities

excitation loop had a miniature 3 dB pad connecting right at the cavity inner wall, while the detection loop had a miniature crystal detector connecting right at the inner cavity wall. Once the nature of the various modes had been determined by probing cavity ends, side walls, and into the drift tube gap, the loop probes were permanently mounted at the opposing end walls. This left the drift tunnel region free for insertion of a small quartz rod to measure Rsh/Q. The perturbing quartz rod was centered by means of plastic centering plugs at the outside drift tube ends.

B. S-BAND CAVITY MODES

Figure 4 is a diagram explaining principal box cavity mode types up in frequency and through and beyond the second harmonic. Five mode types are shown. Three of these may be detected as degenerate modes. For example, when cavity length L is not greatly different from cavity width W, the same type mode may be supported along two different axes, normal to each other, with each component mode having a somewhat different frequency. Thus, the so-called 1-3 mode has a counterpart identified as the 3-1 mode.

The numbers 1-1, 1-2, and 1-3 identify the number of rf variations across the width W and along the length L respectively for the mode in question. RF variations along cavity length L are coincident with the number of half-guide wavelengths, the actual length being modified by tuning effects at the interaction gap. The nature of the various modes is discussed in the following sections.

1. Main (1-1) Mode

The main mode has a strong axial $\bar{E}$ field across the interaction gap and is, of course, the mode with which electron beam interaction is desired. It exists as a half guide wavelength resonance, actual cavity length L being foreshortened by capacitance at the gap. Highest Rsh/Q may be realized in this mode for a large interaction gap and with width W and length L close to

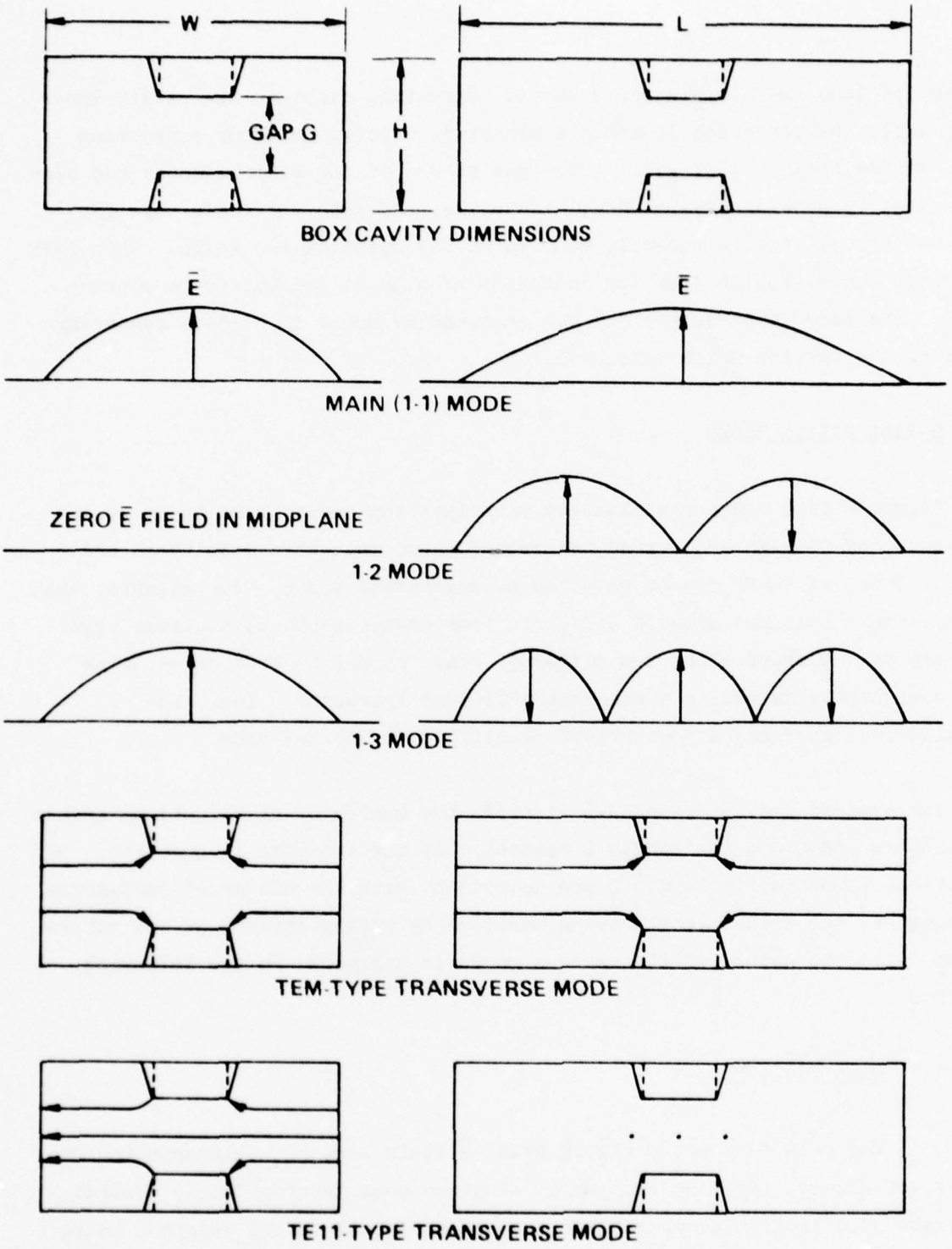

Figure 4. Diagrams Explaining Principal Box Cavity Mode Types

the same size. Cavity height also effects Rsh/Q, smaller heights giving lower values. Mode frequency is a function of all dimensions. Tuning is frequently achieved by use of a movable wall. Preassembly frequency adjustments may be made by use of interaction gap size changes.

2. 1-2 Mode

The 1-2 mode has weak axial $\bar{E}$ fields across the interaction gap. With symmetrical cavity designs, one would expect weak coupling to the mode. The $\bar{E}$ fields are, in addition, of opposite sense from one side of the interaction gap to the other. However, any asymmetry of resonant cavity shape or of electron beam centering within the drift tunnel may result in enhanced mode coupling.

The 1-2 mode exists as the two half guide wavelength resonance. Actual cavity length is modified by tuning effects at the interaction gap. In this case, $\bar{E}$ fields are weak at the gap, while $\bar{H}$ fields are stronger. Hence, tuning is said to be "inductive", and effective cavity length is increased somewhat. The resonant condition is close to that for which the cavity is a guide wavelength, λg, long. Figure 5 is a comparison of observed 1-2 mode frequency in one of the cavities with calculated guide wavelength, λg. Actual cavity length L is somewhat longer at a given frequency than λg, though the difference is not large.

The 1-2 mode frequency tunes rapidly with cavity length L and with cavity width W but responds only slightly to cavity height H or to interaction gap size G.

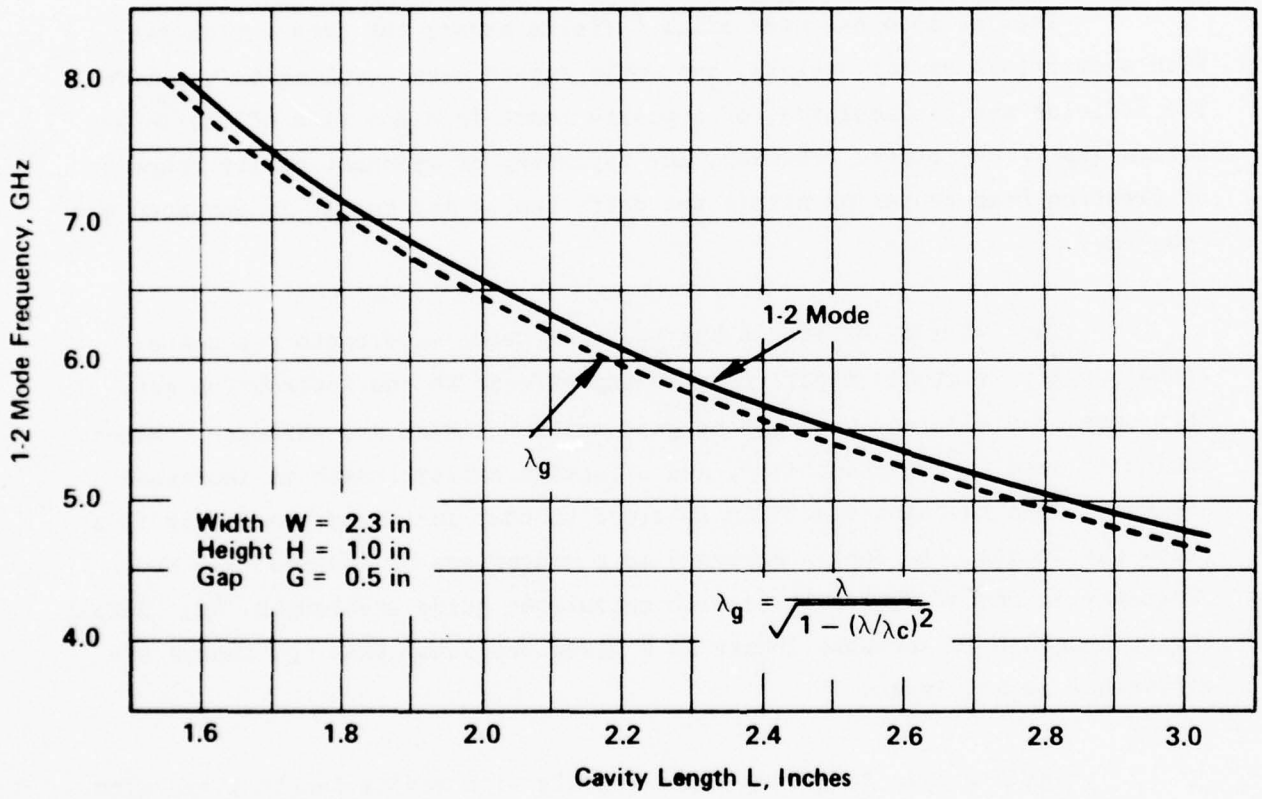

Figure 5. Calculated and Observed 1-2 Mode Frequency vs Cavity Length

3. 1-3 Mode

The 1-3 mode has a relatively strong $\bar{E}$ field across the interaction gap and typically exhibits an Rsh/Q of about half that of the main mode. The mode exists as the three half guide wavelength resonance. Actual cavity length is foreshortened by capacitance at the interaction gap. Figure 6 is a comparison of observed 1-3 mode frequency in one of the cavities with calculated three half guide wavelengths, 1.5 λg. At a given frequency of resonance, actual cavity length L is substantially shorter than calculated length. The topmost curve of the graph shows percentage foreshortening of the calculated length, 1.5 λg, to obtain actual cavity length L at a given frequency. The percentage is plotted against actual cavity length L. For a near box-shaped cavity, a typical drift tube interaction gap, then, would be expected to foreshorten the cavity resonator by about 10%. The 1-3 mode frequency tunes rapidly with cavity length L and with cavity width W. It also tunes with interaction gap size G. But it responds only slightly to cavity height H.

4. TEM Type Mode

The TEM "type" mode is so identified because it is similar to the first coaxial mode. If one imagines a short coaxial line with a shorting plane at each end, a strong resonance exists for which the coaxial line is one half wavelength long. The $\bar{E}$ field is strong at the center of the cavity across or transverse in all directions between the center post and the outer wall. In the klystron cylindrical resonator, cavity height H is identified with the half wavelength dimension. The presence of the interaction gap G moves the TEM type mode frequency higher. If the gap G is made larger and larger, finally becoming equal to cavity height H, the mode becomes the "pillbox" TM_{01} mode at a much higher frequency. Over the possible range of interaction gap sizes in the usual klystron resonator TEM type mode frequency tuning is not large. Cavity height H is the principal frequency-determining parameter.

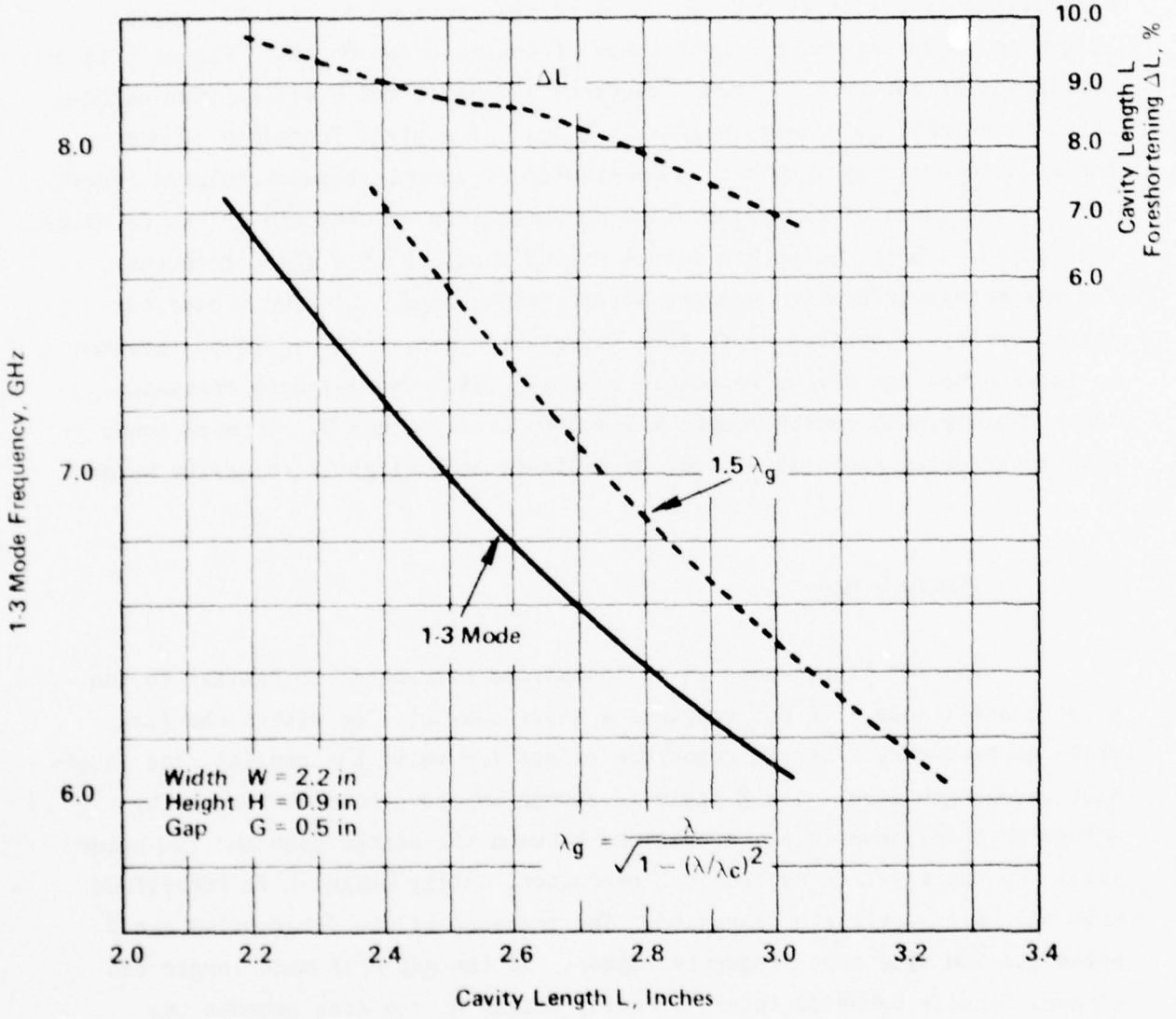

Figure 6. Calculated and Observed 1-3 Mode Frequency vs Cavity Length

In the box-shaped klystron resonator cavity length L has a moderate effect on TEM type mode frequency, though cavity height H has the dominant effect. The TEM type mode usually exhibits a relatively high Q response, and it is probably the most troublesome competing mode to be dealt with in klystron resonator design. The axial component of $\bar{E}$ field shows field reversal in crossing the interaction gap. For this reason, it is sometimes necessary not only to shift the mode frequency out of the second harmonic region, but also to introduce some form of loading to lower the resonator Q of the mode to prevent self oscillation.

5. TE_{11} Type Mode

The TE_{11} "type" mode is so identified because it is similar to the second coaxial mode. If one imagines a short coaxial line with a shorting plane at each end, as with the TEM type mode, a strong resonance exists at a higher frequency for this mode as well. The $\bar{E}$ field is strong at the center of the cavity across or transverse from one side of the outer wall to the other. The presence of the center post does not have a major effect on mode frequency. If it were to be removed, the mode would become the "pillbox" cavity TE_{11} mode at a somewhat higher frequency. Some slight tuning occurs with interaction gap size G over the range of values used in typical klystron resonators; but, again, cavity height H is the principal frequency-determining parameter. In the box-shaped klystron resonator cavity length L has a moderate effect on TE_{11} type mode frequency, though cavity height H has the dominant effect.

6. Higher Frequency Modes

The present study has included modes up to 8.0 GHz in frequency. In proving out C-band cavities it will be necessary to study modes up to about 12 GHz in order to check out possible second harmonic mode competition. Modes exist, of course, in greater and greater profusion as one moves to higher and

higher frequencies. In most cases it is not profitable to study modes much above the second harmonic frequency region. Except for the introduction of loading, for instance, there is little that can be accomplished with a third harmonic competing mode in a broadband microwave tube. Attempts to shift the frequency of such a mode will almost always result in undesirable changes in the more important second harmonic frequency region. In a few cases where third harmonic difficulties have been experienced, mode loading has been employed as a correction.

C. S-BAND CAVITY MODE DISTRIBUTION

Figures 7 through 12 show mode distribution graphs obtained in testing the resonator cavities shown in Figure 1. Figures 7 and 8 show data obtained in initial tests, in which cavity height H was 1.0 inch. The significant factor in these graphs is the presence of transverse modes, TEM and TE_{11} types, within the S-band second harmonic frequency region. It was estimated from the tuning behavior of these modes and from other data available on similar cylindrical cavity modes that a reduction of cavity height H to 0.900 inch would shift the transverse modes upwards just above the S-band second harmonic band limit at 7.0 GHz. The change proved to do just that, as shown in Figure 8, which gives data for cavity S-1A.

Similar results were obtained with cavity S-2A. This cavity had a wider cavity width W. Tests were conducted for three different interaction gap G sizes; 0.600, 0.550, and 0.500 inches. These data are shown in Figures 9, 10, and 11.

The object of the mode distribution measurements was to obtain indication of cavity dimensions likely to lead to freedom from mode competition in regions covering both C-band fundamental and S-band second harmonic frequencies. An additional object of tne measurements was to determine Rsh/Q values concomitant with cavities of these dimensions. As is usually the case,

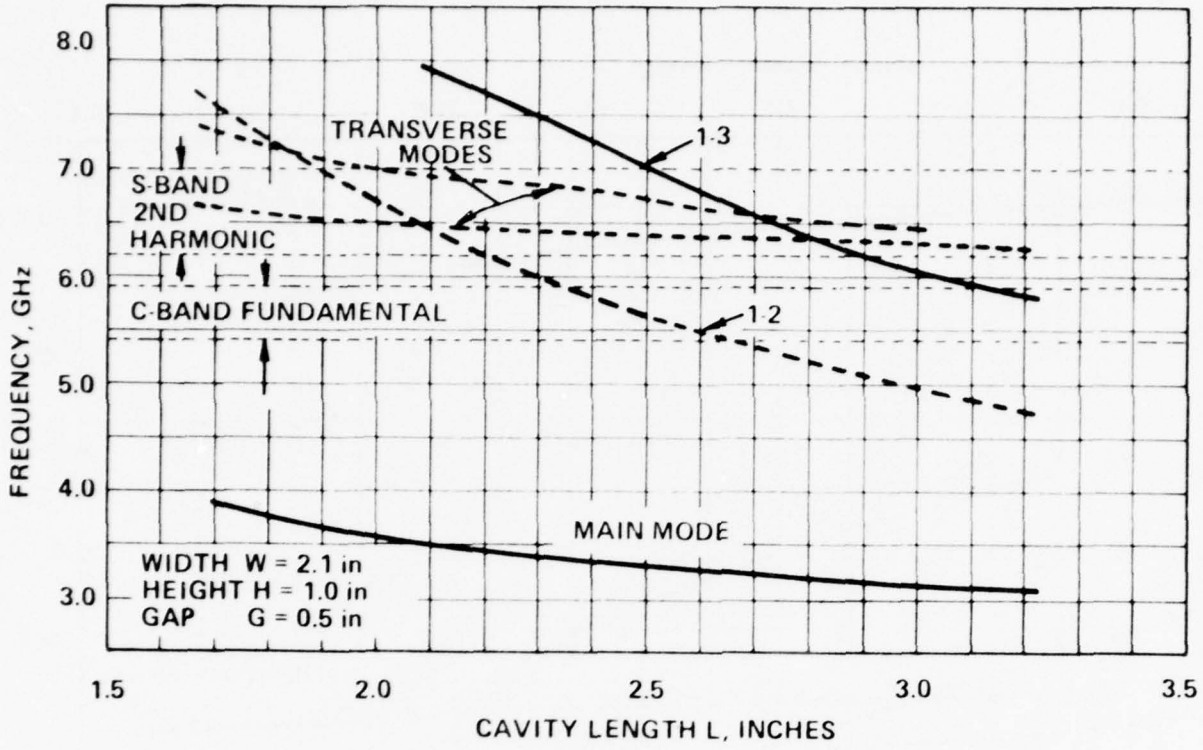

Figure 7. Modes Observed in S-Band Cavity S-1

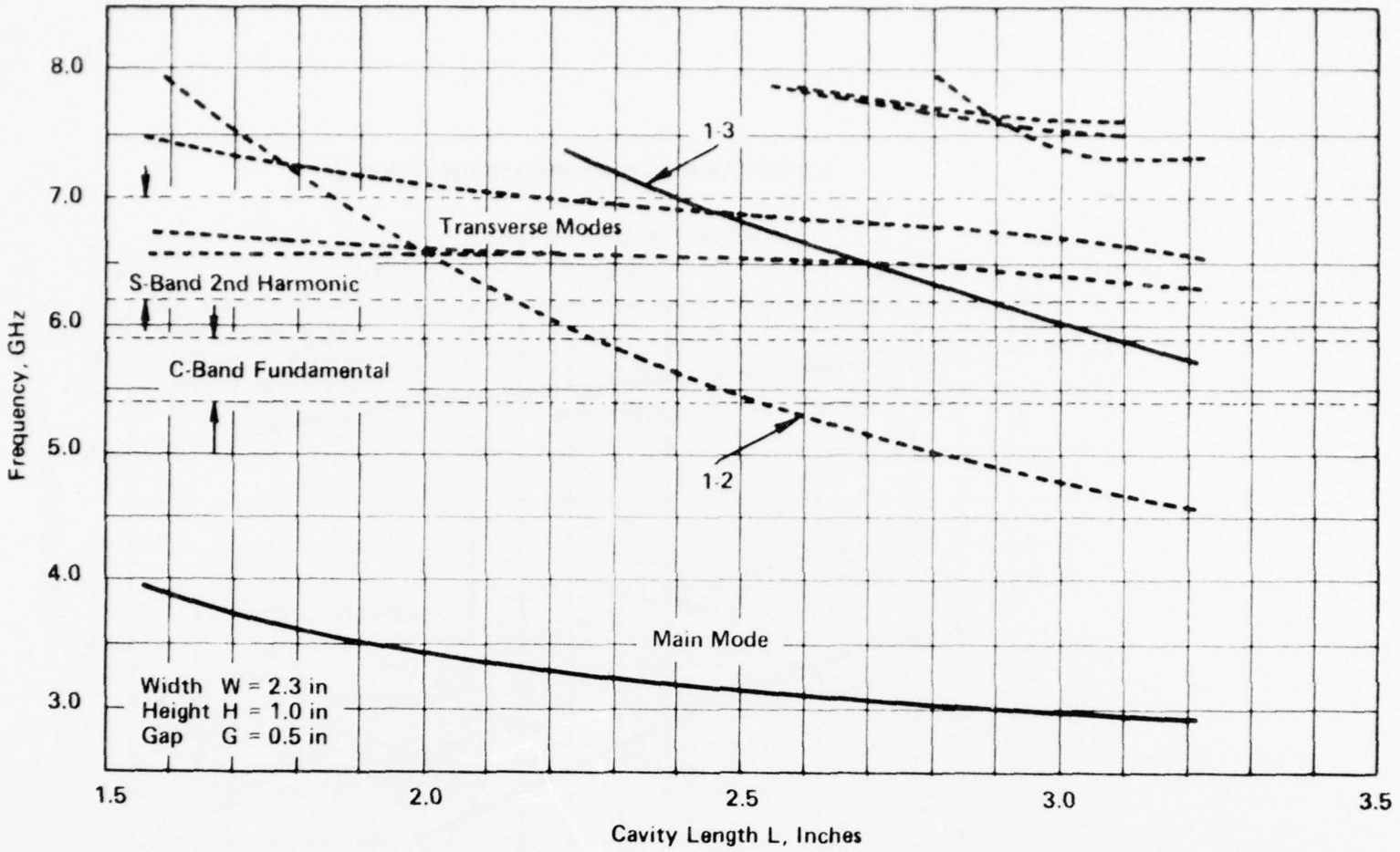

Figure 8. Modes Observed in S-Band Cavity S-3

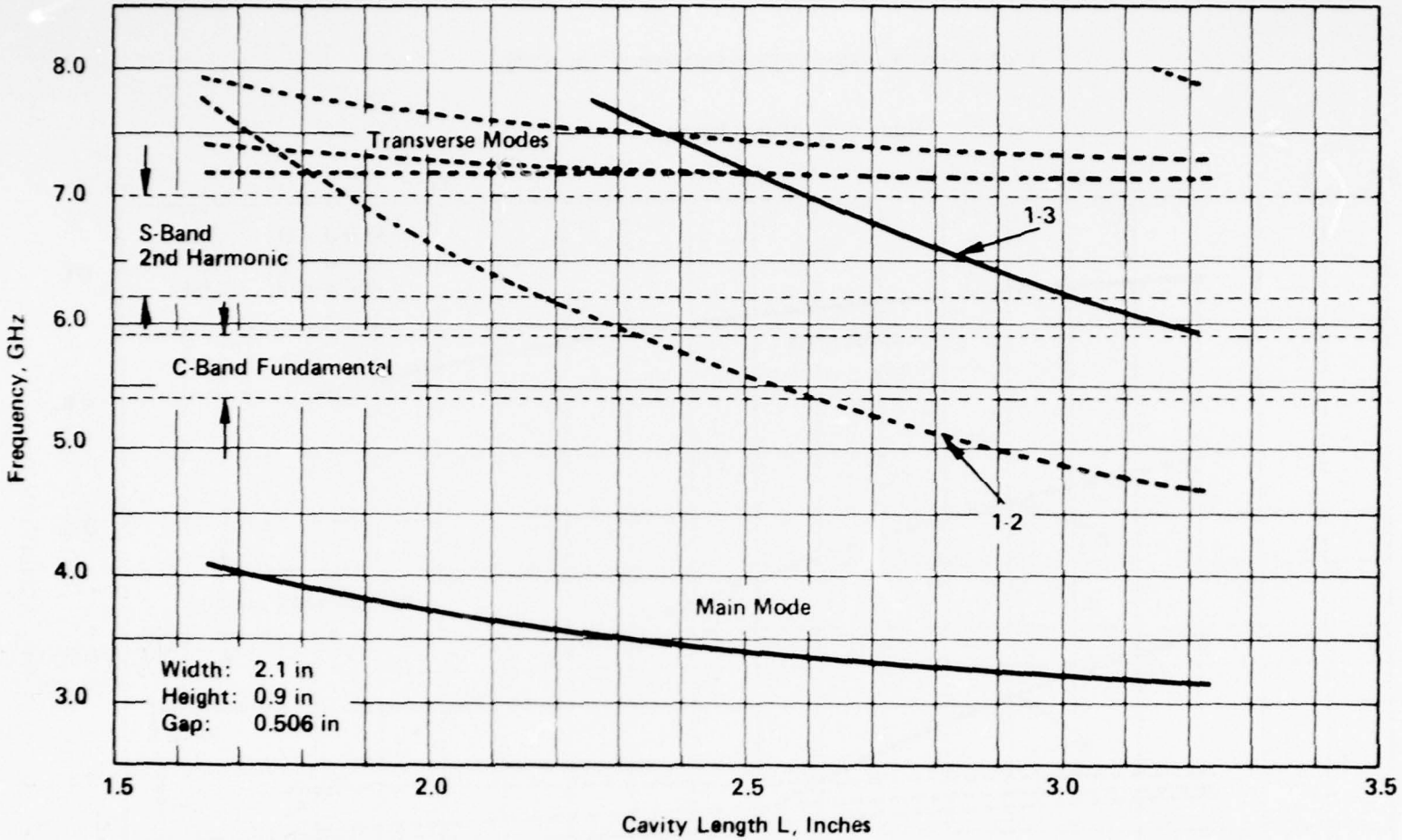

Figure 9. Modes Observed in S-Band Cavity S-1A

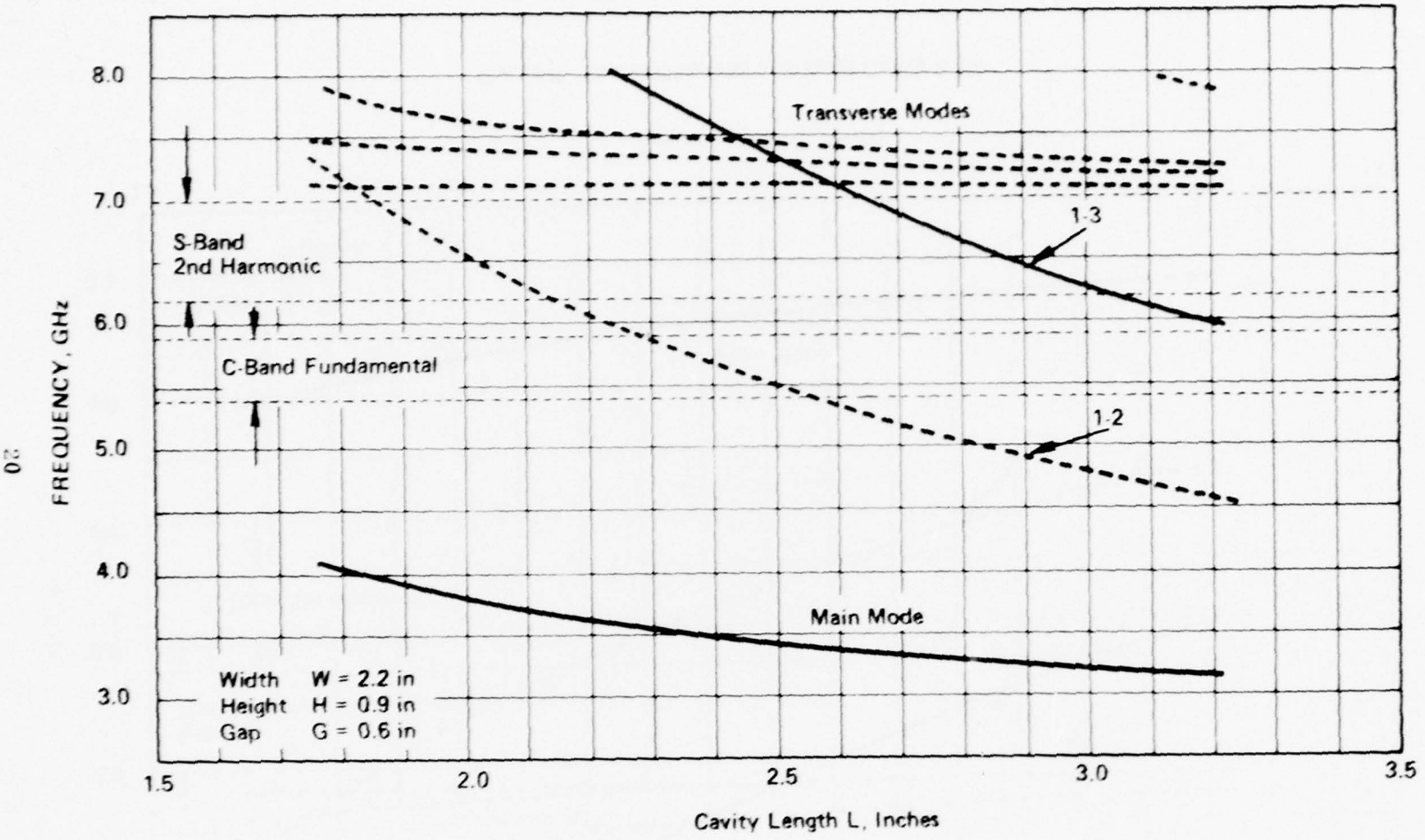

Figure 10. Modes Observed in S-Band Cavity S-2A-1

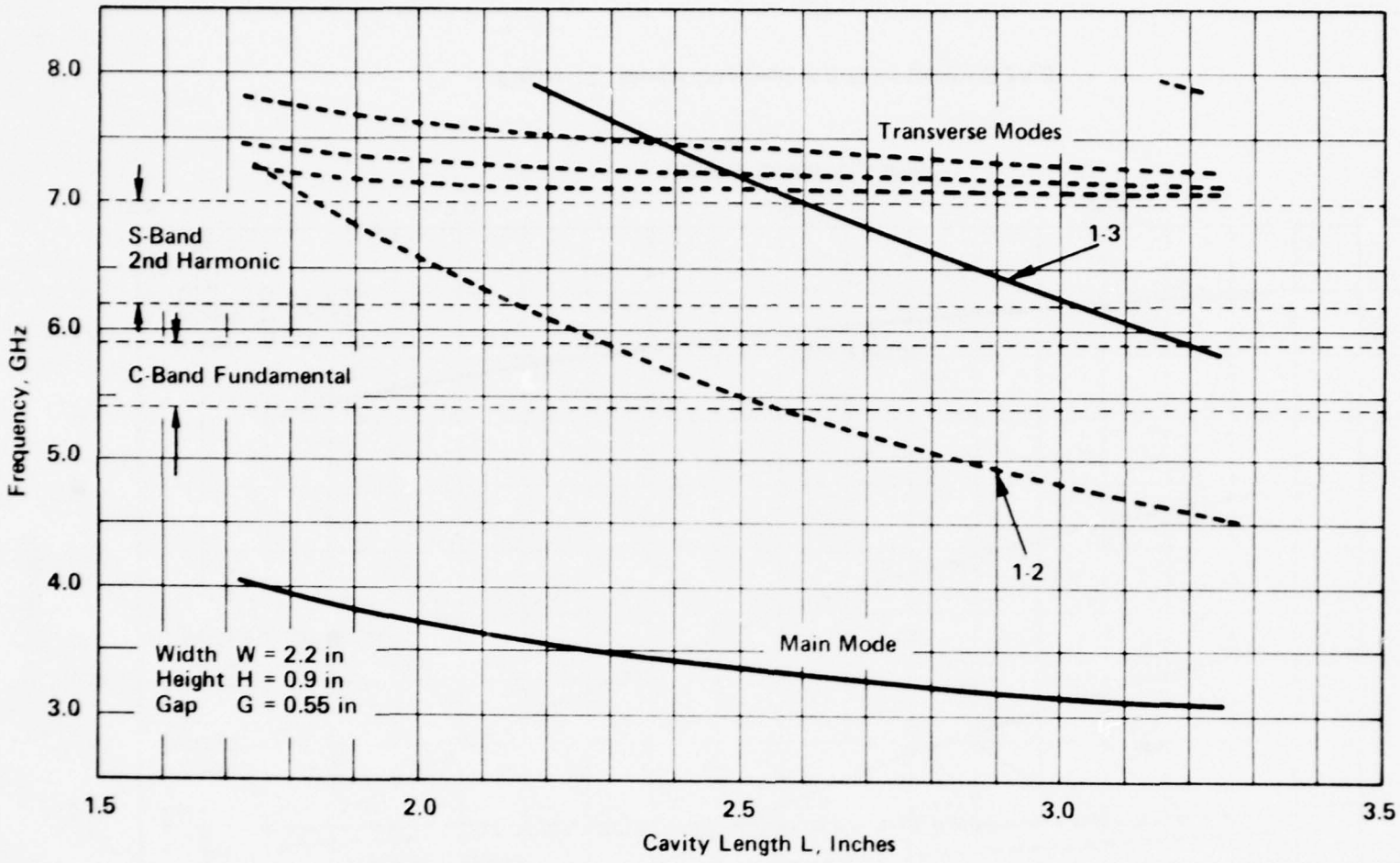

Figure 11. Modes Observed in S-Band Cavity S-2A-2

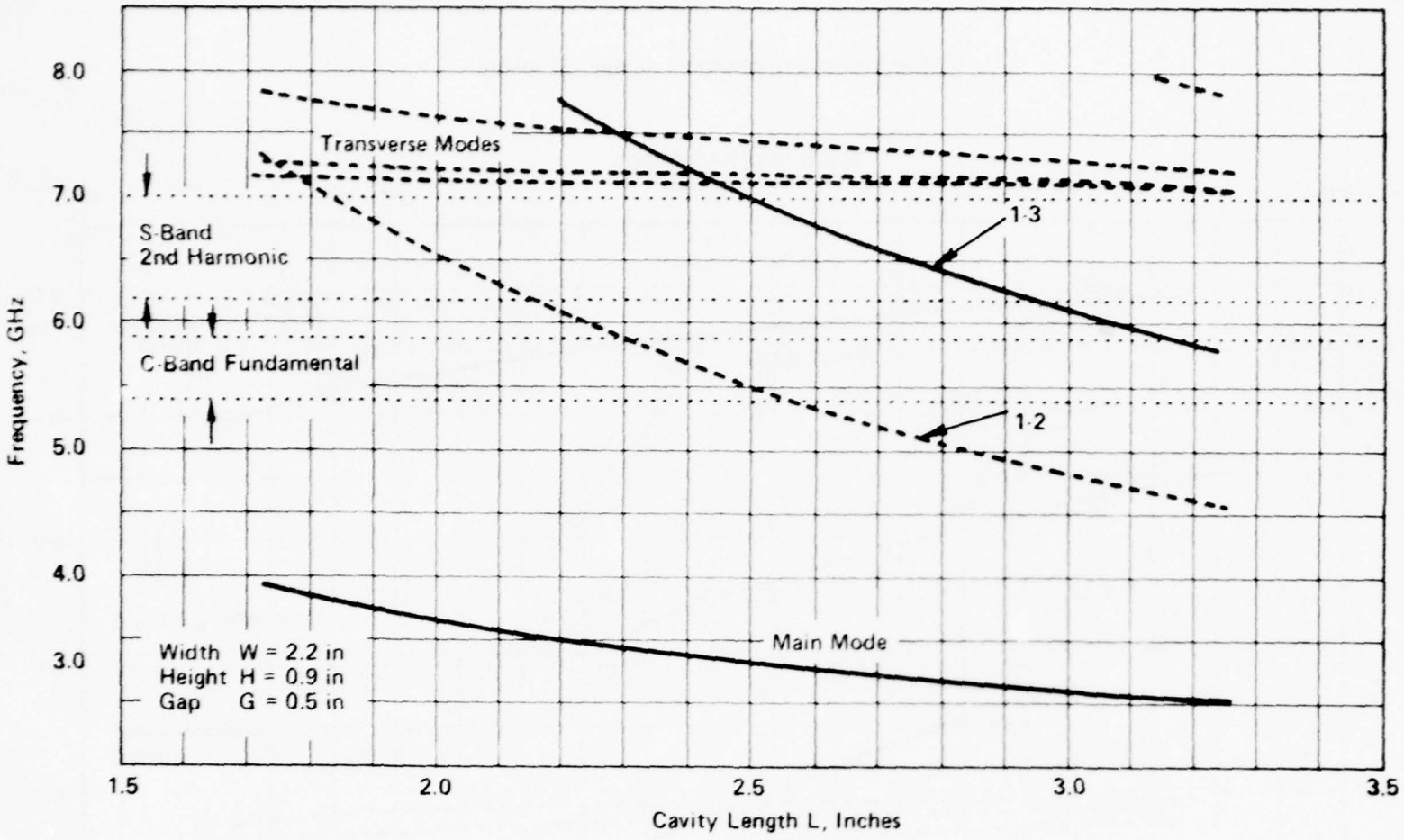

Figure 12. Modes Observed in S-Band Cavity S-2A-3

the attainment of one objective frequently involved some sacrifice with respect to the other. For example, reduction in cavity height H to shift the transverse modes upwards in frequency was accompanied by some reduction in Rsh/Q.

The mode distribution data gave indication of reasonable resonator designs for cavities at high and at midband frequencies, as will be shown later. The indicated possible design for the low frequency cavity, No. 2 in the proposed S-band design, however, left something to be desired. Both the Rsh/Q and the electron beam to cavity coupling factor were somewhat low, leading to a relatively low figure of merit, (M^2Rsh/Q.) It appears that further S-band mode distribution cold test work should be undertaken in connection with cavity No. 2 if hardware implementation is considered. This is discussed in more detail in a later section.

D. Rsh/Q Measurements

An Rsh/Q measurement may be made by observing the change in frequency of a mode when a small diameter low loss dielectric rod perturbation is introduced along the axis of the drift tunnel and across the interaction gap of a resonant cavity. A solution is sought to the expression

$$\text{Rsh/Q} = \frac{1.145 \times 10^{12} a}{(\varepsilon - 1) b^2} \times \frac{\Delta f}{fo^2} \times I\ (d/a)$$

a = drift tunnel radius

ε = rod dielectric constant

b = dielectric rod radius

Δf = frequency shift

fo = unperturbed frequency

I(d/a)= function of (d/a), see Figure 13

d = interaction gap length

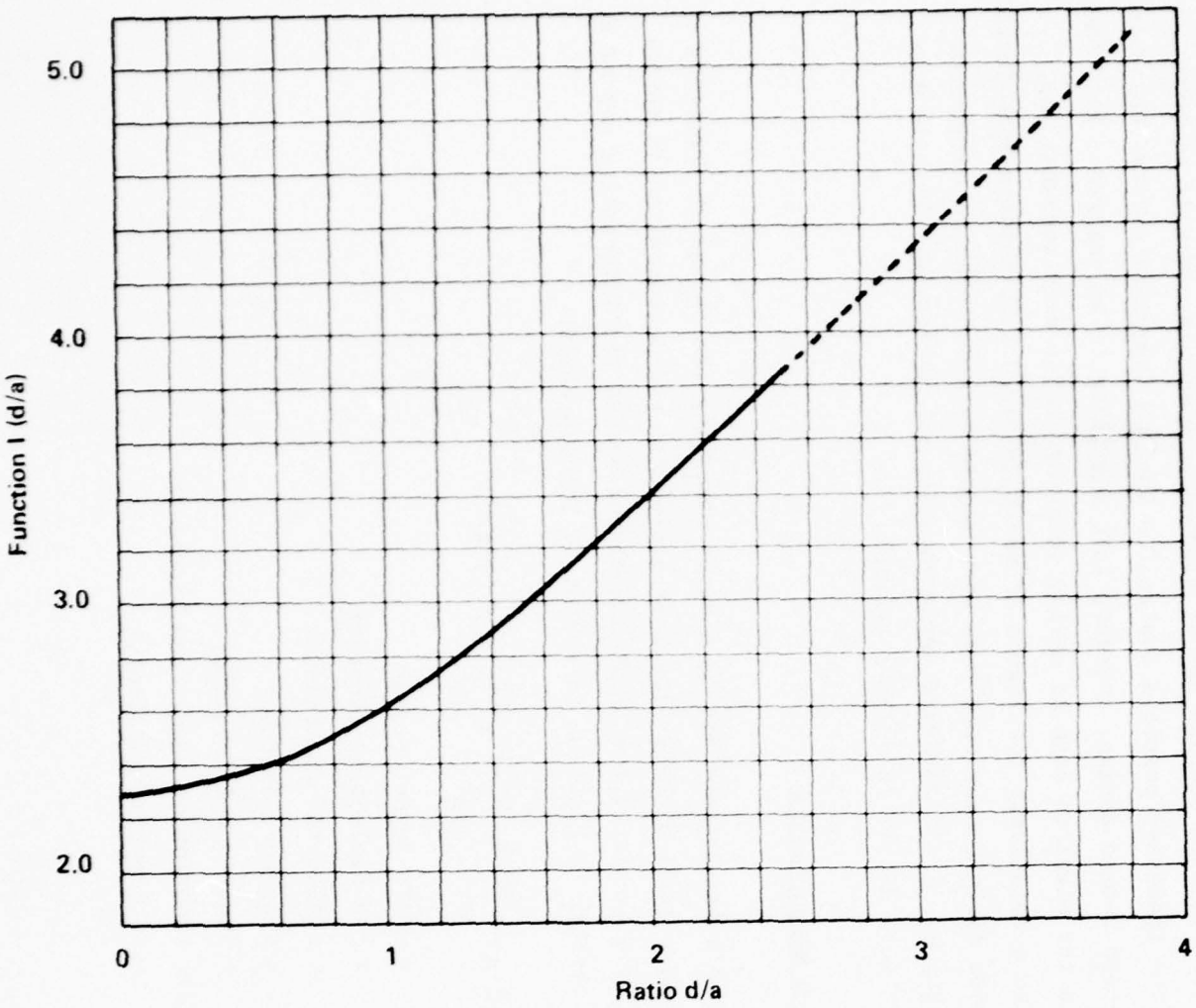

Figure 13. The Function I (d/a) vs Ratio d/a Used in Rsh/Q Determinations

For a given set of physical parameters it is a simple matter to program the Rsh/Q computation on a programmable hand calculator. In a representative program one would first enter the unperturbed frequency, then the perturbed frequency. The program would contain information as to cavity dimensions and physical properties of the dielectric rod, and Rsh/Q would be computed and displayed.

Such a program was used during S-band cavity mode distribution tests to obtain Rsh/Q values applicable to the particular cavity dimensions employed in each test. Figure 14 shows data obtained with cavity S-2A during tests with the three different interaction gap G sizes. Data points are plotted with respect to cavity length L. The frequency increases for shorter cavity lengths, though not indicated on the graph. Figure 15 shows similar data plotted with respect to resonant frequency.

Several tests were made on cavity S-2A for a fixed cavity length L of 1.800 inches with gap G sizes from 0.3 to 0.6 inch. It was desired to determine mode distribution, main mode frequency, and Rsh/Q over the range of gap sizes. The data is shown in Figure 16.

5. Figure of Merit, $M^2 Rsh/Q$

It is not Rsh/Q alone that determines the merit of a particular cavity design. The value of this parameter multiplied by the square of the coupling factor M is the real measure of worth. While Rsh/Q grows larger with increasing interaction gap G size, M decreases. The optimum value of gap size G is ordinarily somewhere near 1.5 radians. A really accurate determination requires a great deal of experimental data, but a useful approximation may be obtained for guidance through equivalent circuit techniques.

With data available as to cavity resonant frequency, tuning vs gap size, Rsh/Q, and coupling factor M for a particular case, one may assume that

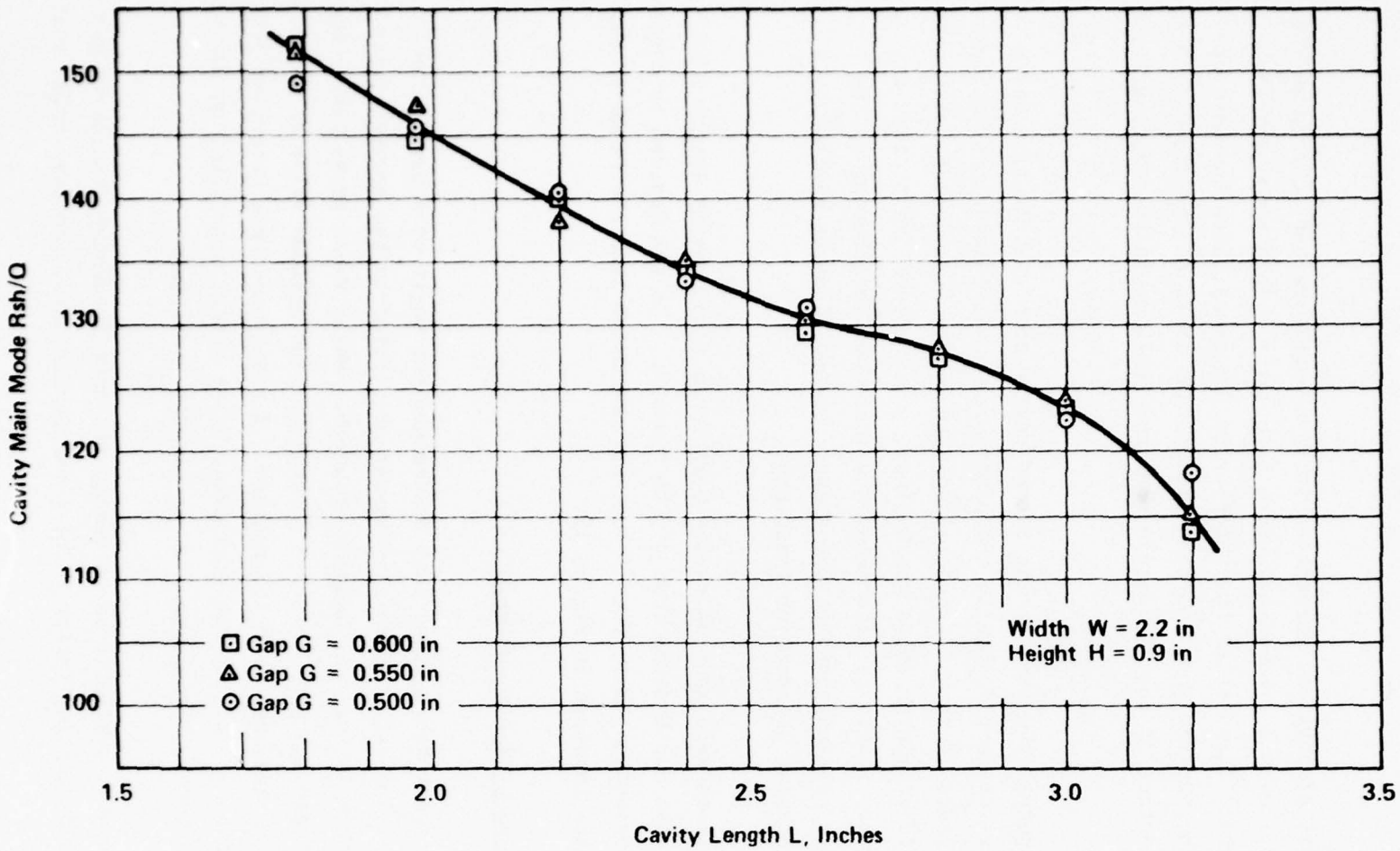

Figure 14. Cavity S-2A Rsh/Q vs Cavity Length

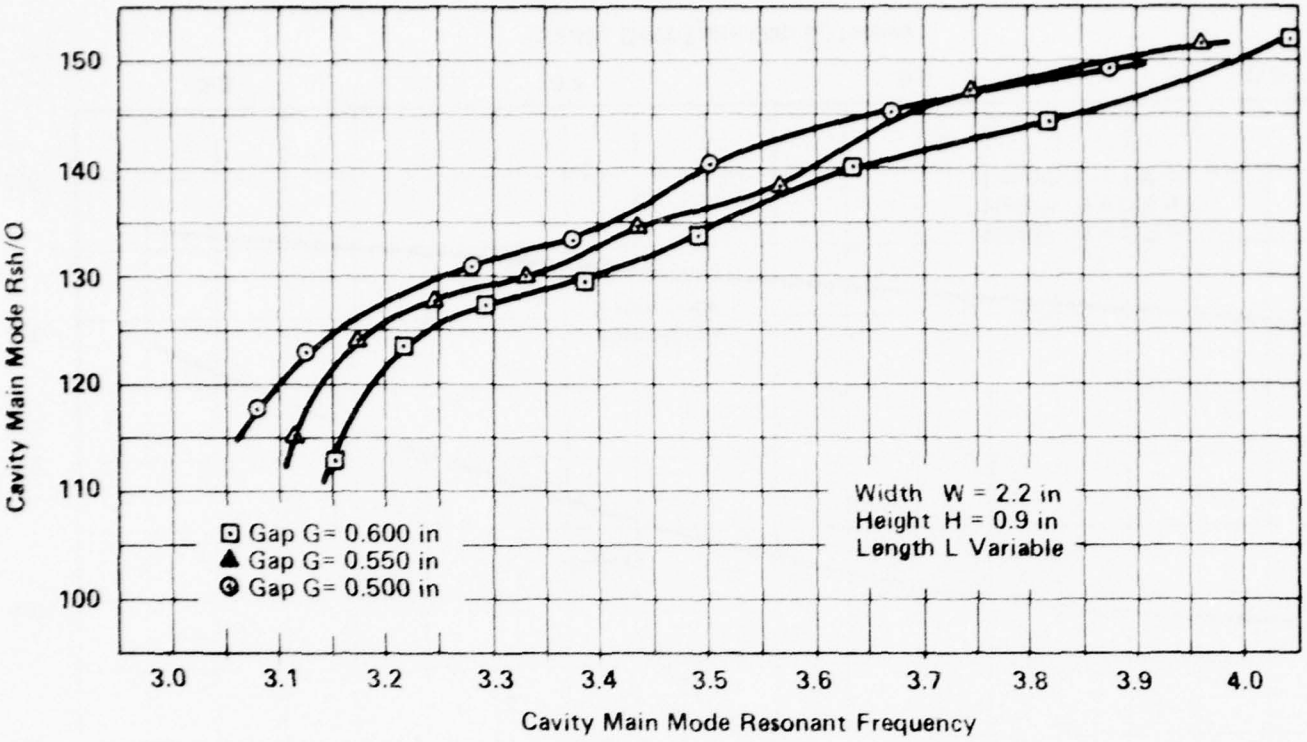

Figure 15. Cavity S-2A Rsh/Q vs Frequency with Gap G as a Parameter

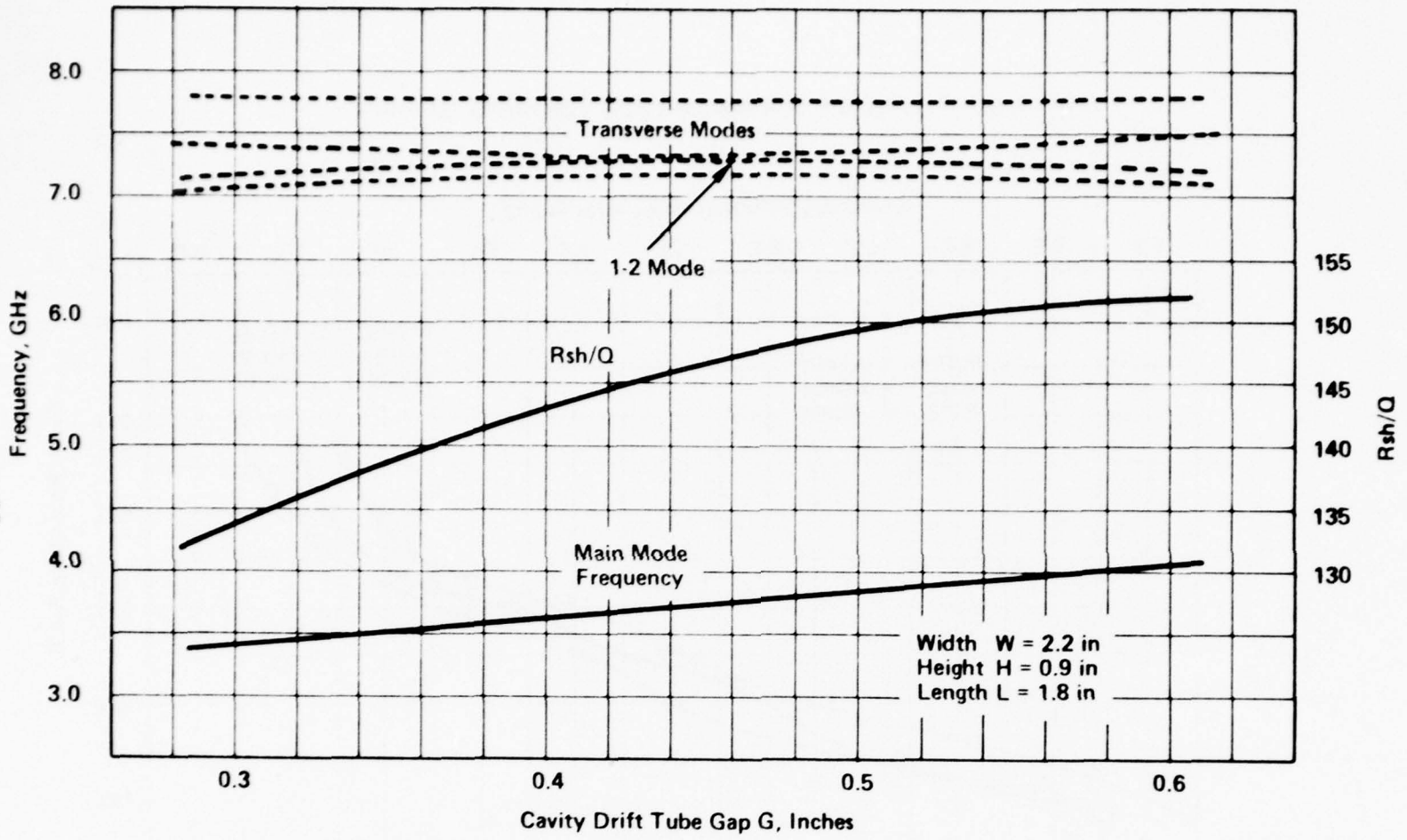

Figure 16. Modes and Rsh/Q Observed in S-Band Cavity S-2A as a Function of Drift Tube Gap

a change in gap size represents only a change in capacity and that an appropriate change in inductance must be employed to maintain resonant frequency constant. One has, for example

$$\omega_1 \cong \frac{1}{\sqrt{L_1 C_1}} \quad \text{and} \quad R_{sh}/Q_1 \cong \sqrt{\frac{L_1}{C_1}}$$

If one now reduces gap size, increasing gap capacitance by 30%, then

$$C_2 = 1.3\ C_1 \quad \text{and} \quad L_2 = 0.77\ L_1$$

Rsh/Q, then, must be changed according to

$$R_{sh}/Q_2 \cong \sqrt{\frac{0.77\ L_1}{1.3\ C_1}} = 0.77\sqrt{\frac{L_1}{C_1}}$$

The factor by which Rsh is changed may be determined from knowledge of resonant frequency tuning vs gap size. For example, in the case above, if only the gap size is changed, changing capacity but leaving inductance constant, then one has

$$\frac{\omega_2}{\omega_1} = \frac{\sqrt{L_1 C_1}}{\sqrt{L_1 C_2}} = \sqrt{\frac{C_1}{C_2}} \qquad \frac{1}{1.3} = 0.77$$

The factor changing Rsh/Q for the new gap size is, therefore, merely the ratio of the new frequency to the original frequency.

Figure 17 illustrates the exercise for an S-band cavity resonant frequency of 3.62 GHz. M has been calculated and plotted as a function of gap size G for appropriate electron beam conditions. Rsh/Q is known for a gap size G of 0.400 inch from Figure 16. Main mode frequency vs gap size may also be taken from this graph. The so-called "corrected" Rsh/Q and the figure of merit, M^2Rsh/Q have been calculated and plotted as a function of gap size G in

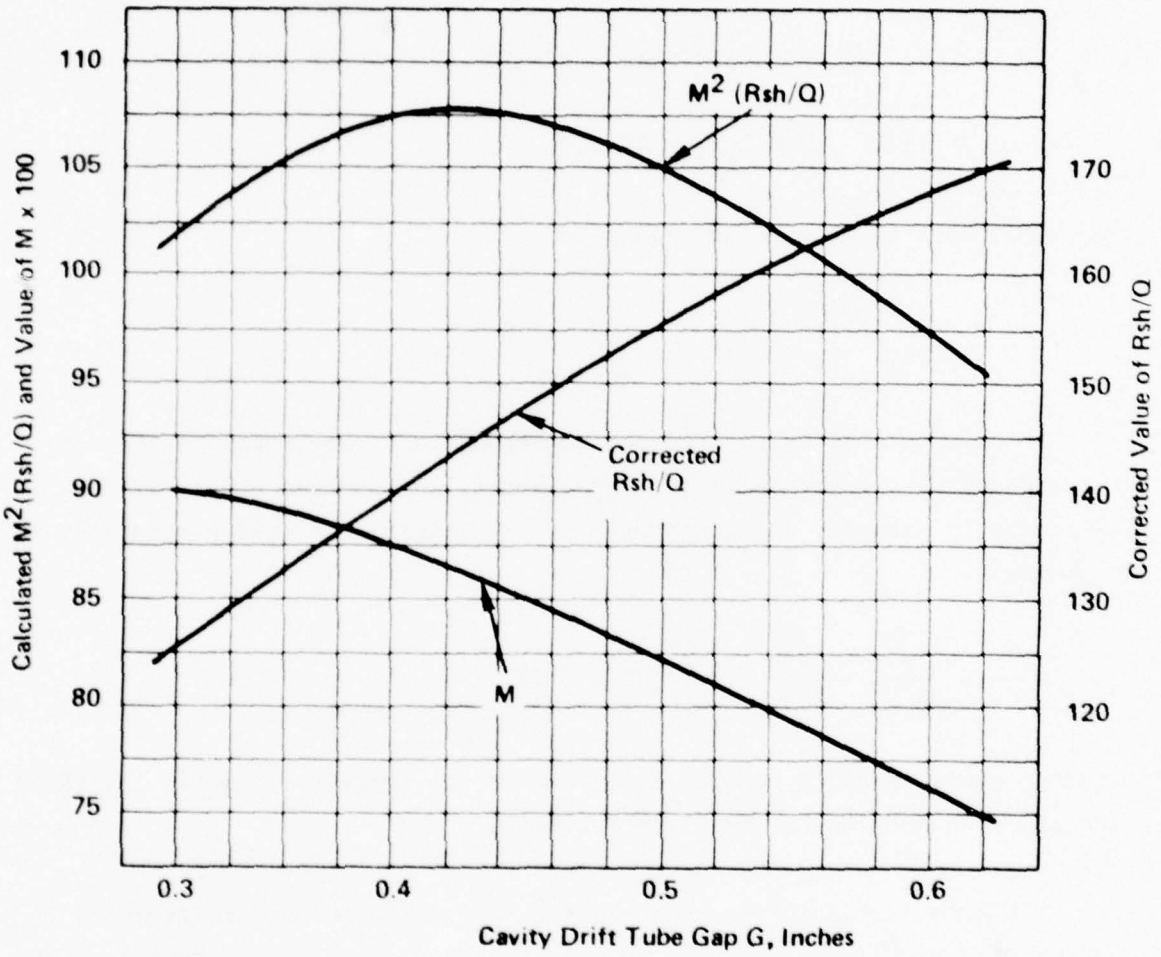

Figure 17. Calculation of M^2 (Rsh/Q) vs Drift Tube Gap Size at 3.62 GHz

accordance with the preceding argument. The optimum gap size G in this case is close to 0.400 inch, equivalent to about 1.3 radians.

The principal weakness in the equivalent circuit treatment is that a so-called change in inductance involves modification of cavity volume, with likely alteration of Rsh/Q from this cause. In other words, it is an oversimplification to take resonator capacitance as existing solely at the interaction gap.

6. S-Band Cavity Designs

The S-band cold test data may lead directly to suitable resonant cavity designs in some cases. Or the data may be used to give indication of possible design solutions at cavity box dimensions not directly explored by test. Figure 18 is an example of the latter case, in which resonant cavity data is extrapolated to determine a possible design solution for cavities at or very near 3.3 GHz. The solution sought, of course, is one giving freedom from mode competition with C-band fundamental and S-band second harmonic frequency regions and, at the same time, giving acceptable values of Rsh/Q and figure of merit $M^2(R/Q)$. In this case known values of cavity length L, 1-2 mode frequency, and 1-3 mode frequency are plotted against cavity drift tube gap size G. The 1-2 mode increases in frequency with both reduced gap size G and reduced cavity length L. The 1-3 mode decreases in frequency with reduced gap size G but increases in frequency with reduced cavity length L. The solution sought in this instance is one in which the 1-2 mode is just above the C-band fundamental frequency region but below the S-band second harmonic frequency region, while the 1-3 mode is just above the S-band second harmonic frequency region. The extrapolation suggests a possible solution for a gap size G of about 0.370 inch. This would be a starting point for further cold tests to make certain of mode frequencies and other data. Changes in cavity length L, gap size G, and/or cavity width W would be employed to optimize cavity design in the new dimensional region.

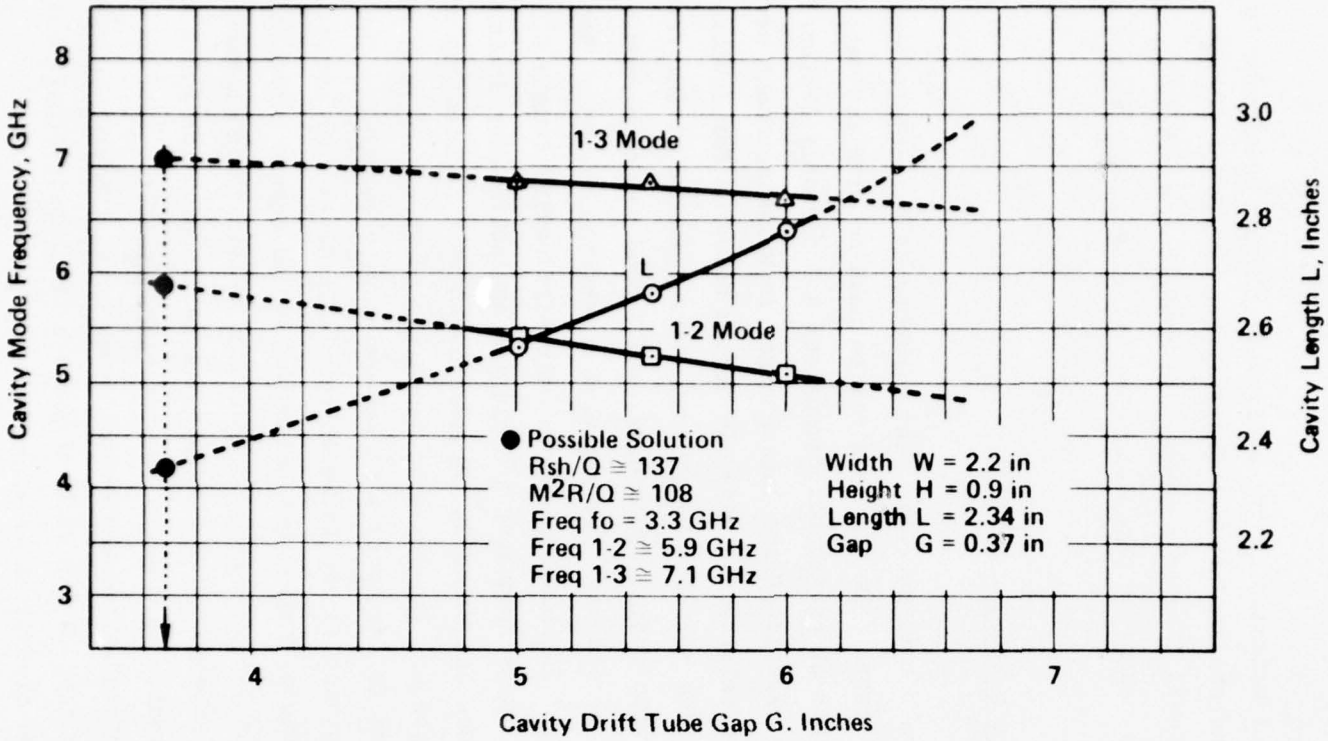

Figure 18. Extrapolation of Cavity Data to Obtain Possible Design Solution at 3.3 GHz

Direct application of data and procedures of this nature have been employed to obtain tentative solutions for S-band cavity structures. The table below shows the results for a typical cavity disposition.

Cavity No.	Frequency GHz	Rsh/Q	$M^2(R/Q)$	Width W"	Length L"	Height H"	Gap G"
1,3,6	~3.30	137	108	2.200	2.340	0.900	0.370
2	3.17	112	63	2.200	3.150	0.900	0.600
4	3.47	137	111	2.200	1.800	0.900	0.330
5	3.60	143	107	2.200	1.800	0.900	0.400

The Rsh/Q and figure of merit $M^2(R/Q)$ for cavity No. 2 are low and may be improved through further cold test work. This cavity is the lowest frequency cavity required. An experimental cavity of substantially wider width W, for example, may lead to a more desirable solution.

IV. COMPUTER WORK

Heavy dependence is placed on computer results as a guide in klystron design. Six different computer programs were used in the present study effort, and a great many klystron configurations were considered. The total bulk of large signal computer results, for example, is a stack of 11 x 15 inch computer paper sheets some 28 inches high. Most of these data represent solutions not useful for klystron design, though often indicating desirable directions for further study. Some indicate reasonable klystron designs. All of the computer data is preserved for possible reference in any hardware implementation. The six programs mentioned are as follows.

Program	Main Purpose	Data Computed, Characteristics
KDC	Mathematics	Electron beam parameters, interaction gap coupling factors, etc.
GBW	Gain-Bandwidth	Small-signal gain-bandwidth, multi-frequency, single cavity structures, engineering estimates
CPLCV	Gain-Bandwidth	Small-signal gain-bandwidth, multi-frequency, coupled-cavity structures, sophisticated solutions
DBLCV	Large-Signal	Power output and efficiency, single frequency, distance stepping
TCAV	Large-signal	Power output and efficiency, single frequency, time stepping
DTC	Output System	Impedance vs frequency, synthesizes characteristics

KDC makes rapid calculations giving pertinent electron beam characteristics, interaction gap coupling factors, and other data for a given set of input parameters. These data may then be used in further computations in other computer programs.

GBW is a relatively simple small-signal-gain-bandwidth program giving reasonable engineering estimates for the input parameters employed. It is arranged to handle single cavity resonant structures along the electron beam, though coupled-cavity approximations may sometimes be obtained through simulation by use of modified input parameters.

CPLCV is a sophisticated small-signal gain-bandwidth program giving relatively accurate results for parameters describing coupled-cavity input and/or output circuits, and other single cavity resonant structures, along the electron beam.

DBLCV and TCAV make large-signal computations at a single given frequency for a specified rf drive power. Hence, it is necessary in the use of either program to make repeated runs at different rf drive power levels to determine indicated saturation characteristics. Moreover, for a broadband klystron it is further necessary to repeat computer runs of this nature for each frequency of interest. In early work, typically three frequencies are studied, near band edges and at band center. Later, as a final design solution is approached, five frequencies are often considered.

DBLCV is a distance stepping program. RF time and phase changes are dependent variables, distance along the axis the independent variable. One cycle of rf is examined, with the assumption that all other cycles are identical. Electron reversal is not permitted. The program is rapid and relatively inexpensive to use.

TCAV is a time stepping program. Electron position along the axis is the dependent variable, time the independent variable. Points along the axis considered must often encompass more than one-half wavelength. Electron reversal is permitted. The program is larger and more complicated than DBLCV, takes considerably longer to run, and is more expensive to use.

DTC will synthesize output system parameters from a desired impedance vs frequency characteristic used as input. The user may then judge if these parameters are realizable in practice. Alternately the program will compute output system impedance for input parameters Rsh/Q, frequency and Q of beam-coupled cavity, frequency and Q of series coupled filter cavity, and cavity-to-cavity iris coupling factor.

Figures 19 and 20 show CPLCV small-signal gain computations for S-band and C-band. Figures 21 and 22 are examples of plots of output system impedance vs frequency for the two bands. A representative set of DBLCV computations for S-band saturation characteristics gave the following results:

CPLCV Case 1538, Output No. 66

Frequency GHz	Gain dB	po MW	η_t %
3.14	35	4.0	33
3.30	34	5.2	42
3.46	35	4.6	39

Similar data is shown for C-band in graphical form in Figure 23.

The saturation data for each case indicate the difficulty of achieving uniform performance across the frequency band. This is attributed to the choice of frequency for the penultimate cavity. As bandwidth becomes wider, it is more and more difficult to attain uniform efficiency. The effect of a single penultimate cavity, tuned inductively to a point above the high frequency end of the

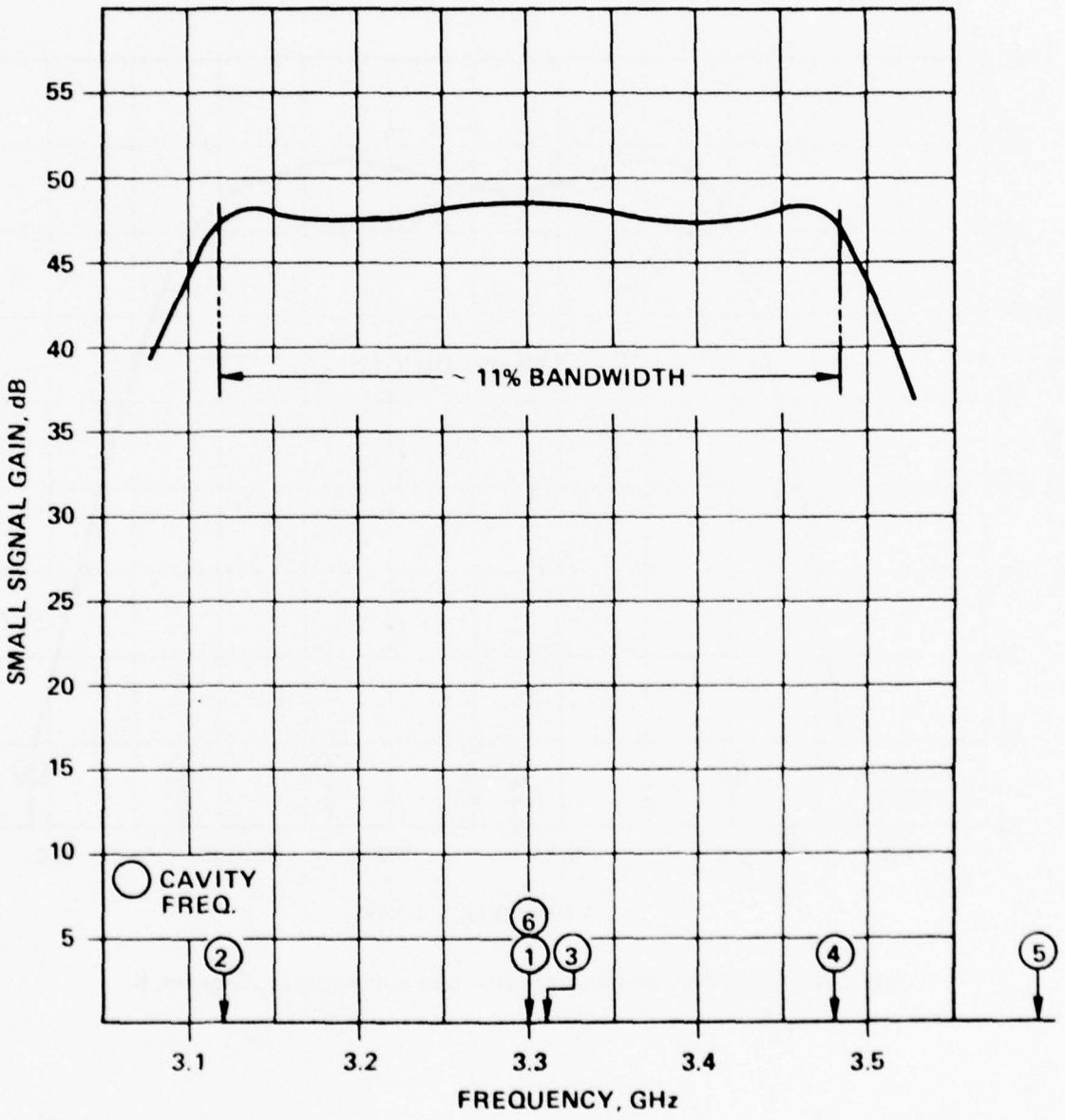

Figure 19. CPLCV S-band Small-Signal Gain vs Frequency, Case No. 1003

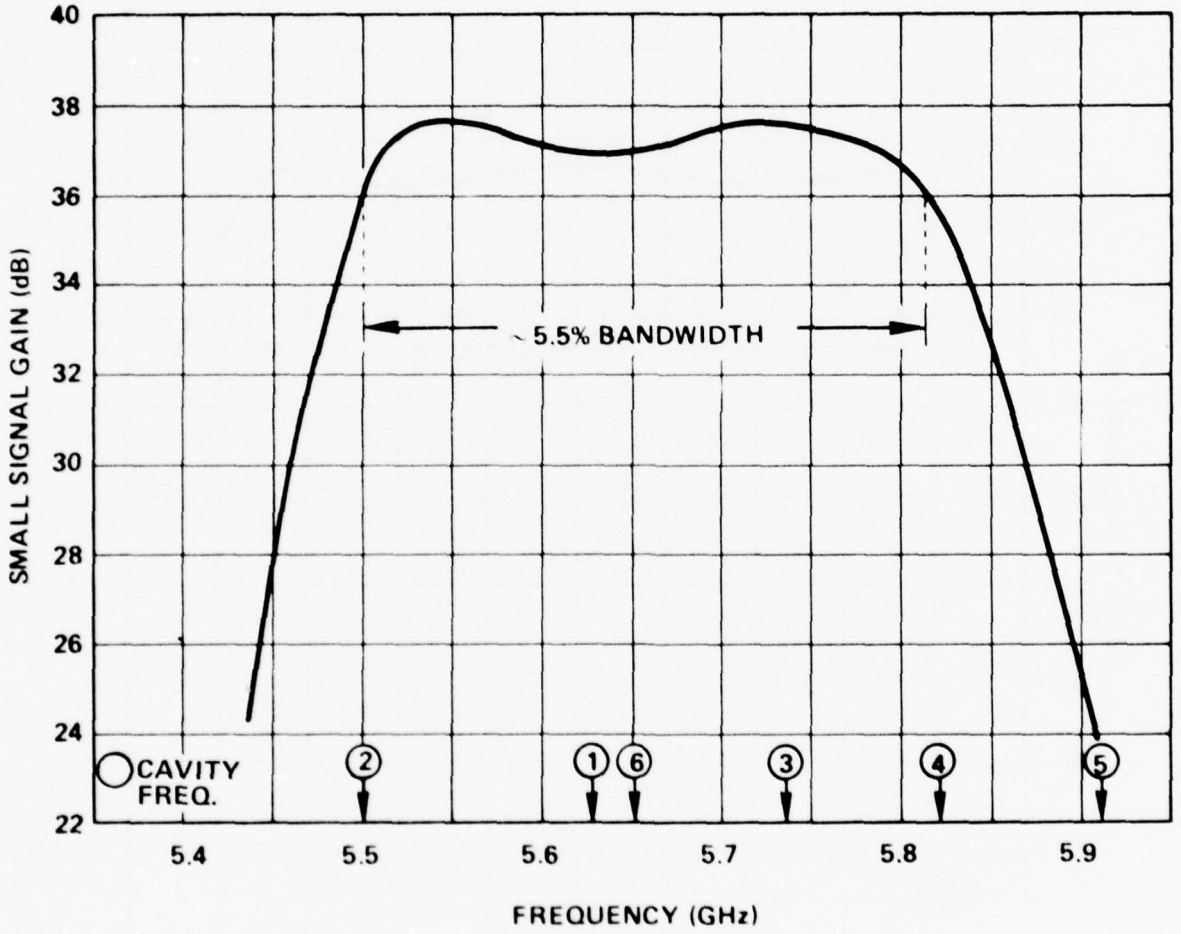

Figure 20. CPLCV C-Band Small-Signal Gain vs Frequency, Case No. 6

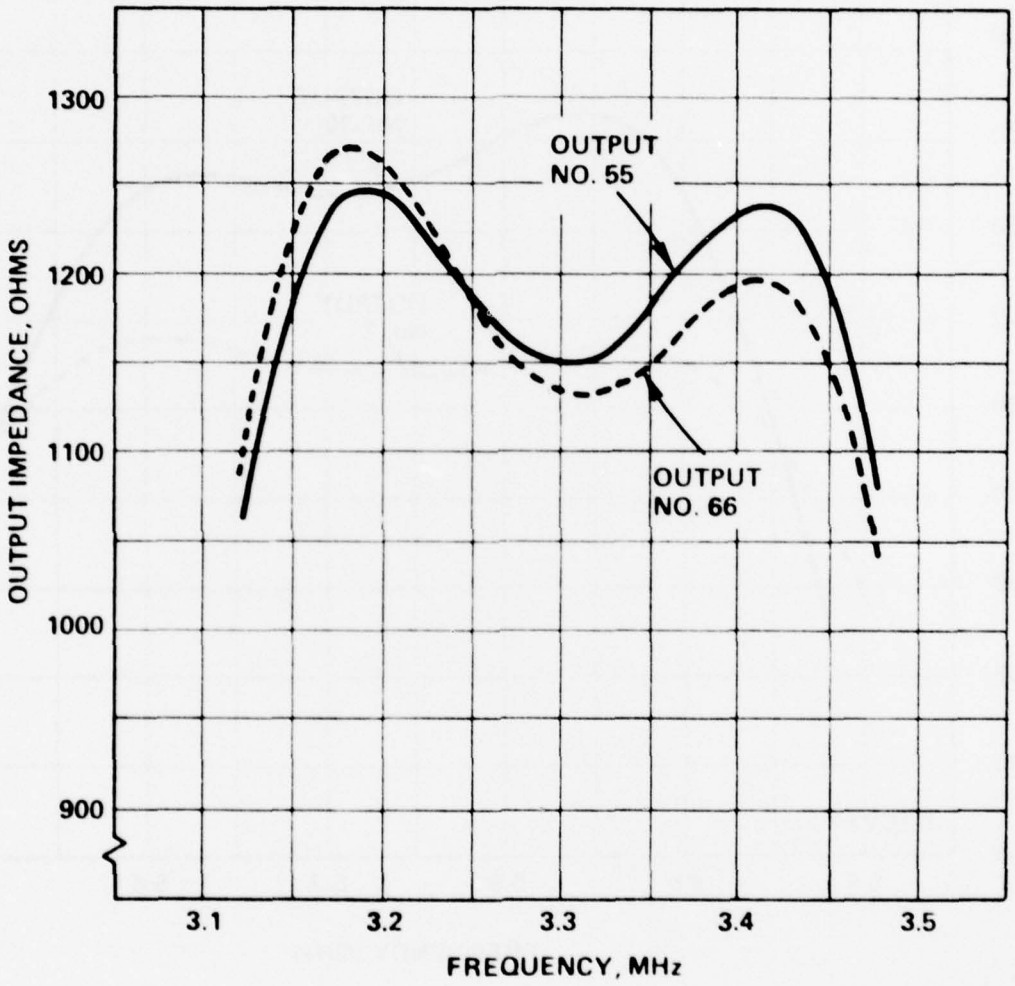

Figure 21. Examples S-Band of Output Impedance Characteristics

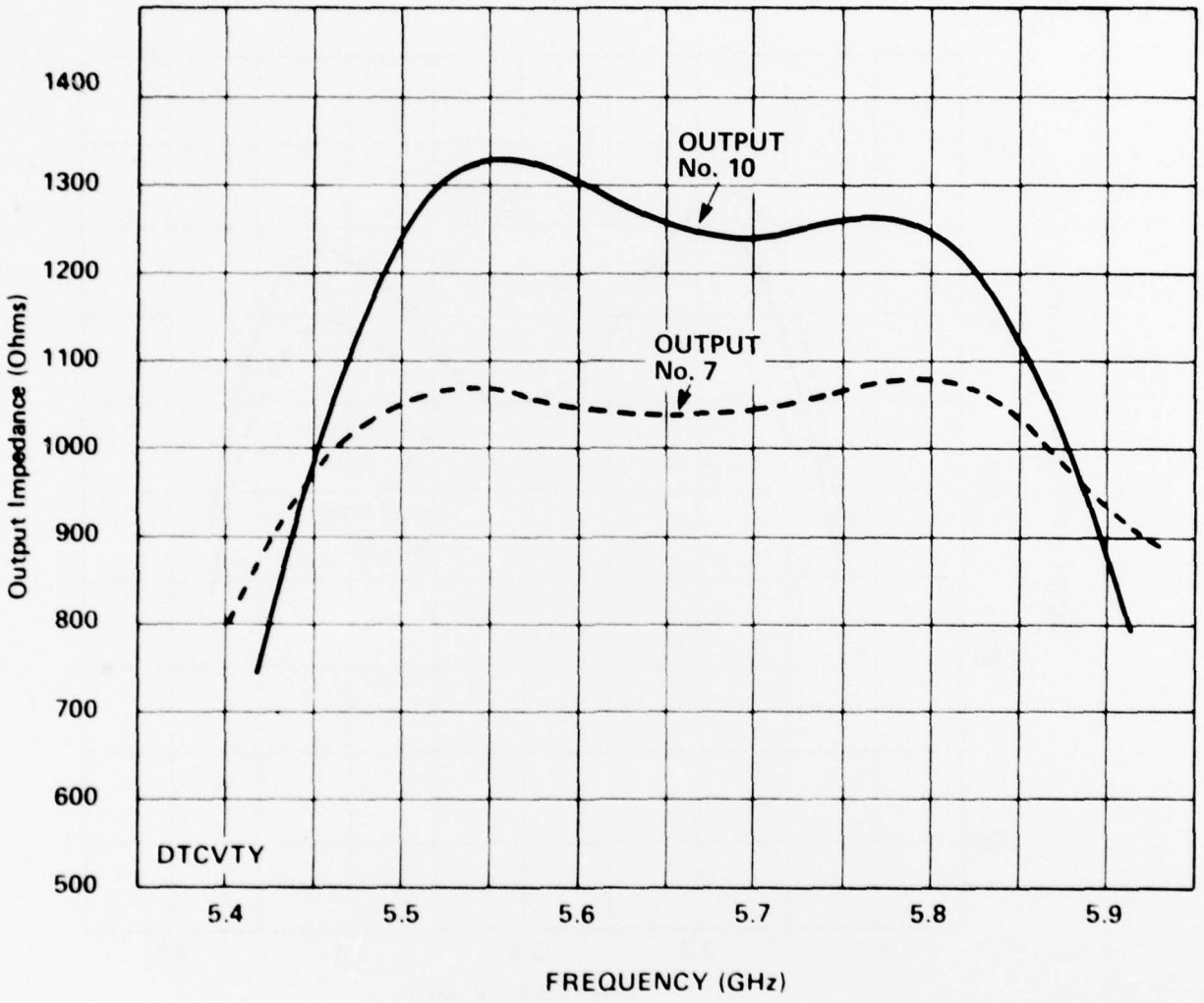

Figure 22. Examples of C-Band Output Impedance Characteristics

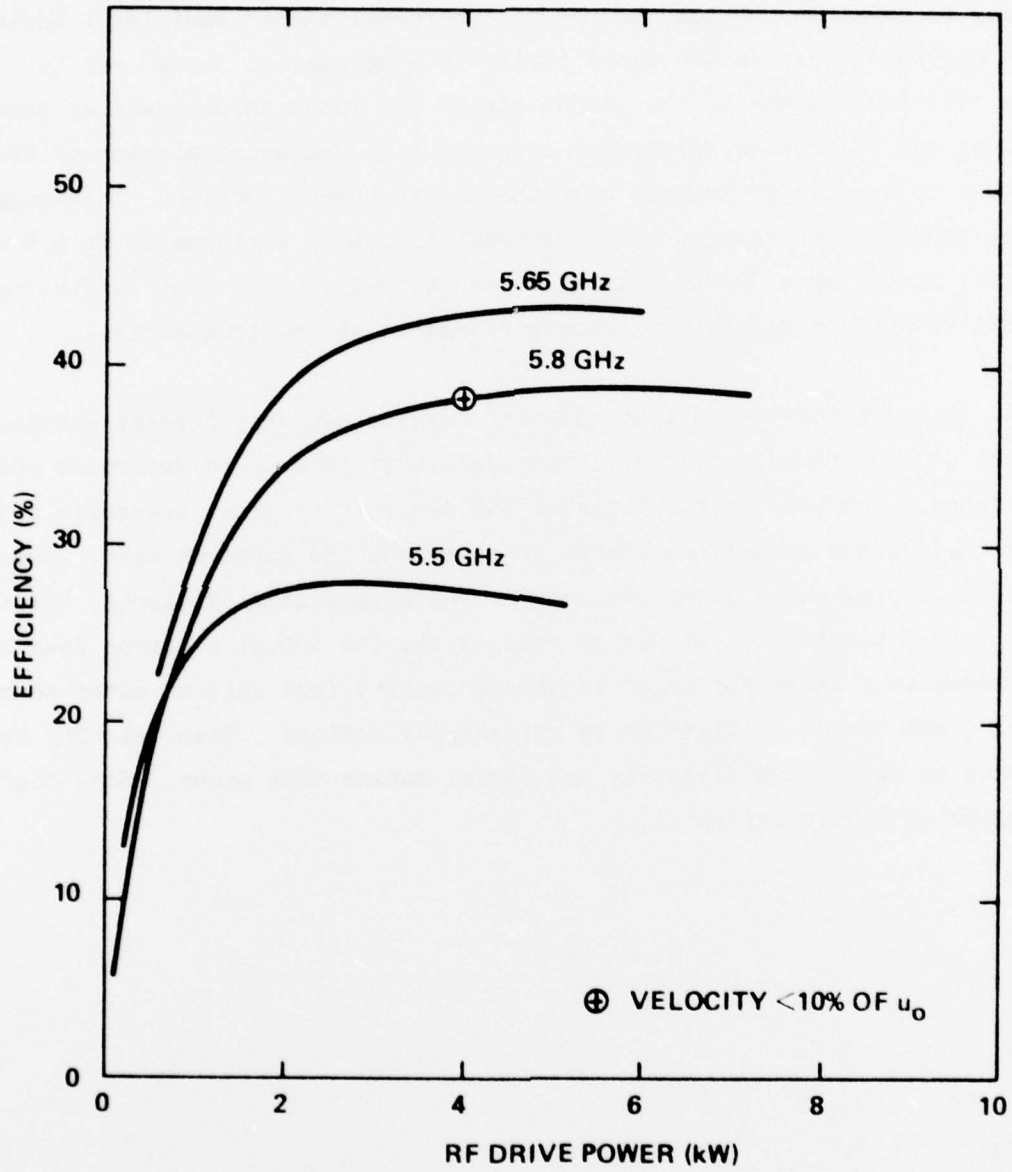

Figure 23. DBLCV C-Band Efficiency vs Rf Drive Power, Cases No. MBC-4, MBC-5, and MBC-6

band, tends to be minimal over the low frequency portion of the band. Improvement may be possible through the use of two "penultimate" cavities. While there may be only one "next to the last" cavity in a mechanical sense, yet two cavities may be positioned close to the output cavity and tuned inductively as penultimate cavities, one to improve efficiency over the high frequency portion of the band, the other to improve efficiency over the low frequency portion. This suggestion will be studied with respect to improvement in C-band performance at 5.5 GHz. Moreover, it may be a useful ploy at S-band as well, where some difficulty has been experienced in maintaining good performance at low frequencies.

It is to be remembered that computer results can only present guidance in klystron design procedures, real tube models must be used to determine actual performance. The practicable large signal computer programs presently available employ rigid discs of uniform charge to represent the electron beam. These move as non-scalloping units along the axis of the mathematical klystron. Radial motion is not permitted. By way of comparison, the actual electron beam usually shows moderately large variation in charge density from axis to outer beam diameter, and the outer diameter is not sharply defined. Beam velocity varies from axis to outer beam diameter, and radial motion does occur. Some degree of scalloping is always present.

V. BEAM STICK EXPERIMENT

The beam stick experiment was set up to attempt, in turn, narrow band klystron operation in two different cavity modes; the main (1-1) mode and the 1-3 mode. Three-halves wavelengtn waveguide resonators have been used in local or test oscillator circuits in the past[1] because the 1-3 mode provides excellent tuning. Two to one frequency ranges may be covered. So it was known that klystron operation in the 1-3 mode is feasible.

Tne Varian 3KM3000LA klystron makes use of a "beam stick" arrangement, the resonant cavities being external box-shaped structures, each designed to separate into nalves and to clamp around tne interaction gap region. Vacuum is provided by a cylindrical ceramic sleeve around each of the three interaction gaps. This klystron was selected for use in the experiment because of availability. It appeared that slight modifications of the resonant cavity boxes would permit cold test study of the modes. As it turned out, it was also necessary to modify and reprocess the basic beam stick structure.

Figure 24 shows the resonant frequency of main (1-1) and 1-3 modes vs tuner dial reading. Figure 25 snows Rsh/Q vs frequency for the main (1-1) mode. Three series of Rsh/Q measurements were made of the 1-3 mode, each with a different interaction gap configuration. It proved necessary to make use of a centered interaction gap to realize an acceptable Rsh/Q in the 1-3 mode. Figure 26 shows data for the tnree tests. Since the standard beam stick used in the 3KM3000LM klystron makes use of two offset interaction gaps, it was necessary to disassemble and reoperate the structure. A preliminary computer check with the GBW program indicated 42 dB small-signal gain in the main (1-1) mode and 29 dB small-signal gain in the 1-3 mode with the centered gap arrangement. Figure 27

---

[1] Reich, Ordung, Krauss, Skolnik; "Microwave Theory and Techniques", pp 487-488, Van Nostrand, 1953

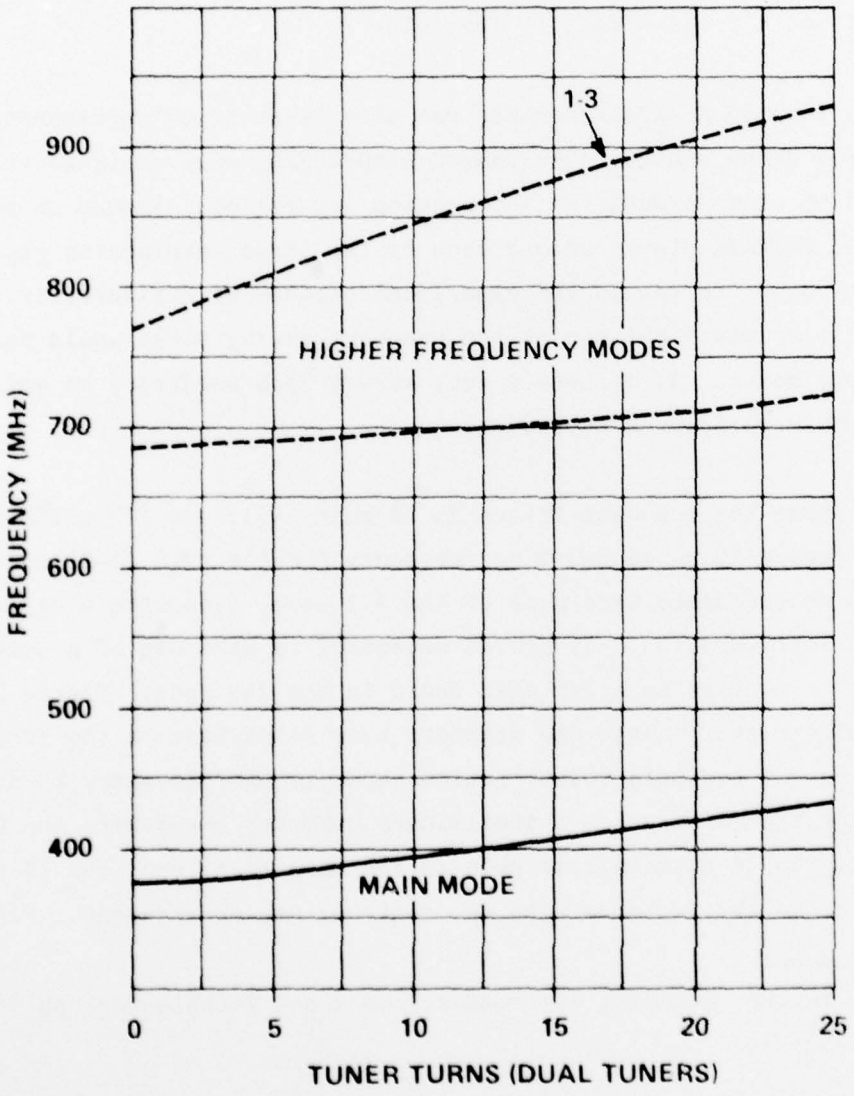

Figure 24. Resonant Modes of the First Cavity of the 3KM3000LA Klystron used as the VA-842 Driver

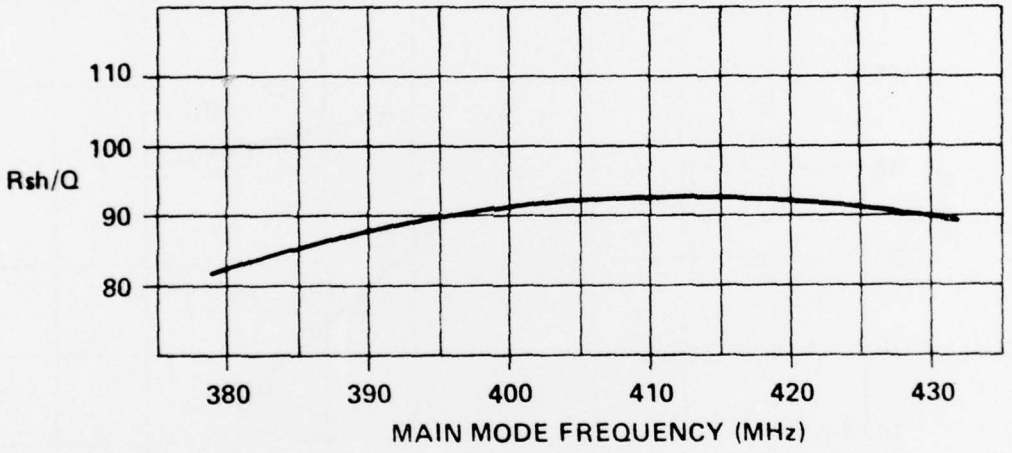

Figure 25. Rsh/Q Measurements Made of Main Mode of the First Cavity of the 3KM3000LA Klystron

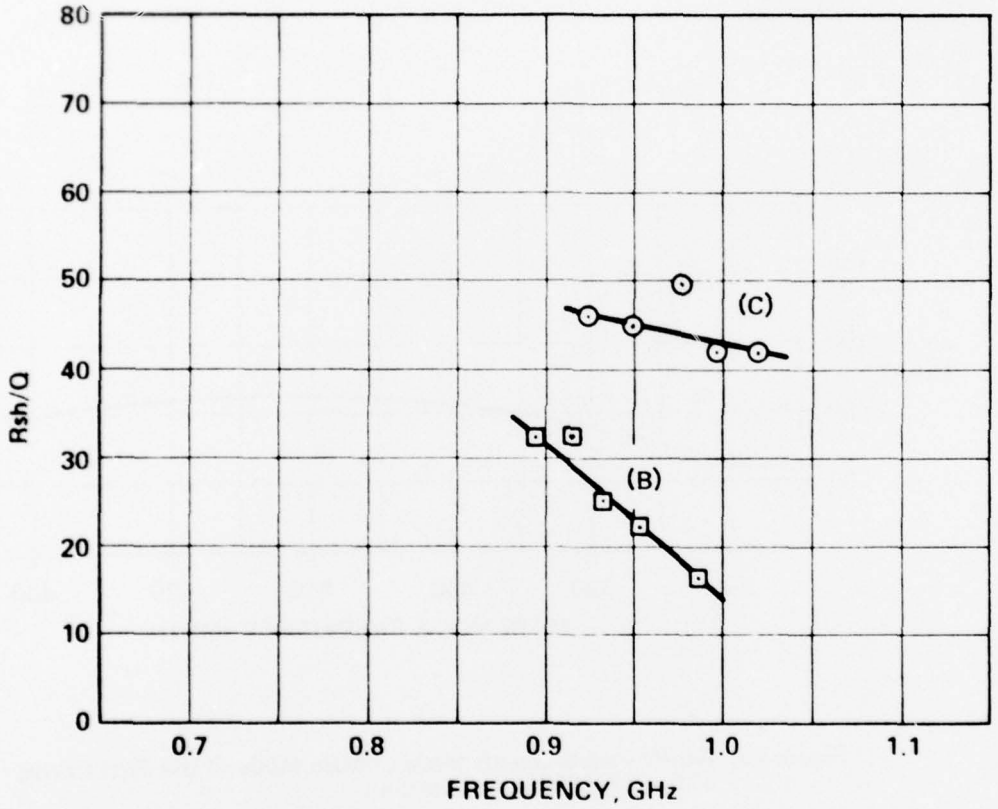

(A) STANDARD CONDITIONS BUT WITH C PLATE AND INSULATING POSTS REMOVED – NOT MEASURABLE

(B) STANDARD CONDITIONS BUT WITH CENTERED GAP

(C) CENTERED GAP AND C PLATE AND INSULATING POSTS REMOVED

Figure 26. Rsh/Q vs Frequency for the 1-3 Mode of the 3KM3000LM Klystron

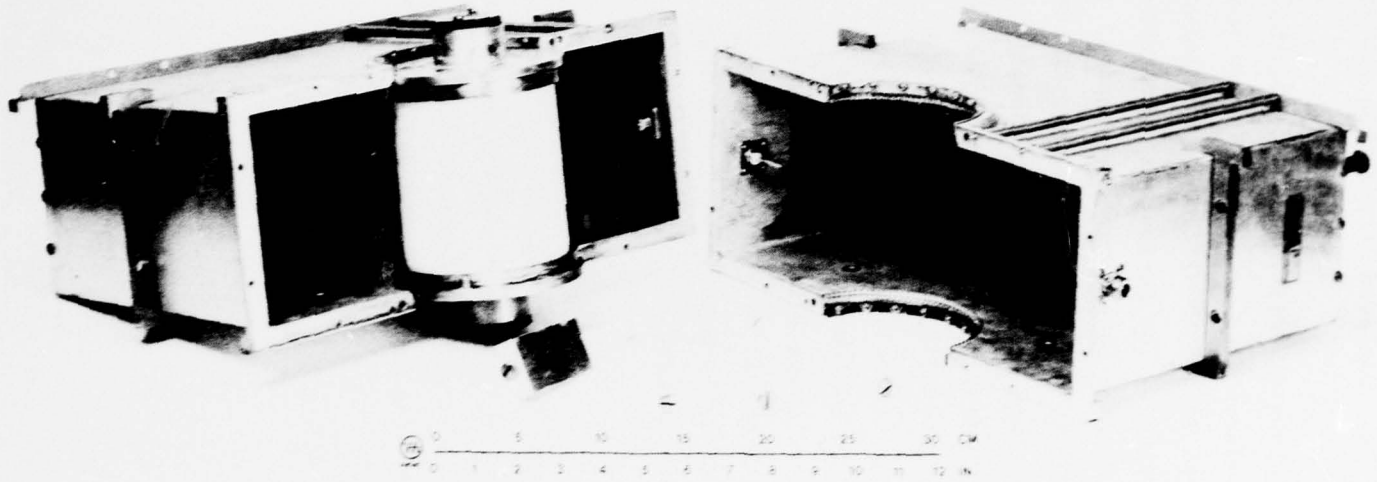

Figure 27. Beam Stick Experimental Cavity

shows an opened box cavity and a ceramic-enclosed interaction region. Figure 28 shows drift tubes used in the standard offset interaction gap arrangement at the left and a set of modified centered interaction gap drift tubes at the right.

In test the experimental klystron showed somewhat lower than normal cathode emission despite extensive aging. Saturated power output in the main (1-1) mode was 1.68 kW, as opposed to the specified 2.0 kW minimum saturated power output for the 3KM3000LM klystron. The device was synchronously tuned in a higher frequency mode, as indicated by resonance responses. Small probes and crystal detectors were used for this purpose. However, klystron performance in this mode was poor. Power output was too low to be measured with normal production water load techniques, and coaxial output couplers in the correct size were not available. Further, doubt existed as to the mode to which the klystron was tuned. It was felt that frequency calibrations established earlier in individual cavity bench cold testing might not be applicable in the real tube. If it were the 1-2 instead of the 1-3 mode, power output should have been low. At the time, it was decided that cold tests should be performed using the modified beam stick and the box cavities to determine the mode to which the tube was adjusted. This could not be accomplished at the test socket at the time because of the pressure of production schedules.

The beam stick experiment, though interesting, has little bearing on the main objectives of the study program, regardless of the outcome. The Rsh/Q's measured in all tests on 1-3 mode responses have been much too low for practicable use of this mode in a broadband microwave tube design.

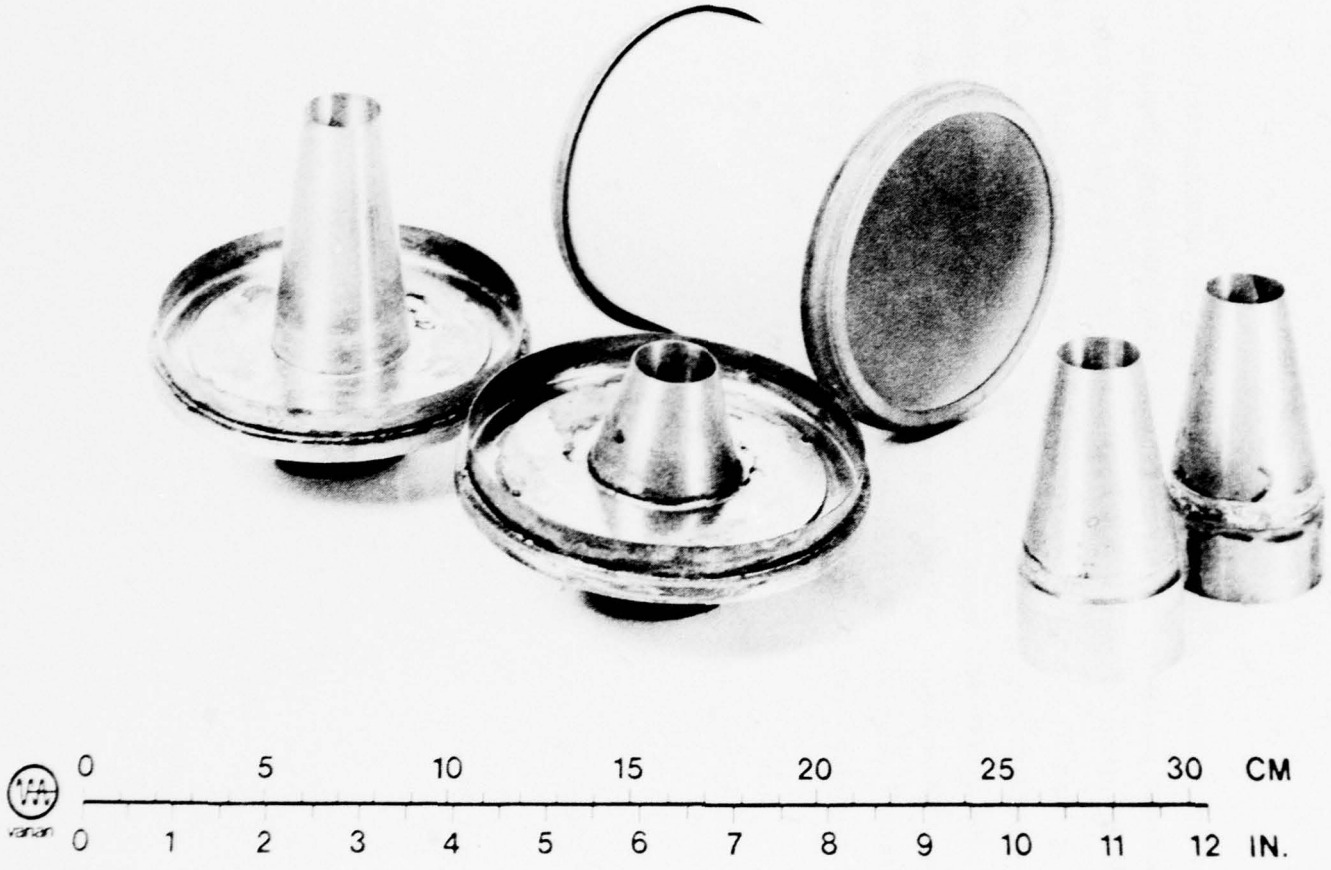

Figure 28. Drift Tubes and Ceramic Support Cylinder

VI. CONCLUSIONS

The present study indicates that a reasonable interspersed S-band and C-band cavity broadband multiband klystron is feasible. Current computer results for the individual bands suggest a 10% operating band at S-band and approximately a 5% operating band at C-band. Separate inputs and outputs would be employed. A microwave waveguide coupling unit external to the tube would be used to direct the rf outputs of the two bandwidths down a single waveguide transmission line to the antenna. There would be two rf driver chains, each connected to the appropriate rf input terminal. RF frequency diversity and rf drive switching would be accomplished at low signal level at a common point in the system.

VII. RECOMMENDATIONS

A single radar having wide-range multiband frequency diversity could be designed using separate S-band and C-band linear beam devices. For two-band operation there would be two tubes. The rf output systems would be combined through use of a microwave waveguide coupling unit, as previously described. Two rf input driver chains would also be employed, as mentioned earlier. Each of the tubes would use a gridded gun, and the appropriate device would be switched on with each rf drive pulse. The advantage derived from this approach would be design optimization at each frequency band and use of the widest possible bandwidth in each device. For example, the C-band Twystron® amplifier VA-913 is capable of 4 MW peak power output over close to a 10% operating bandwidth. Present day broadband C-band klystrons are capable of but half this bandwidth. Five percent is the projected C-band bandwidth for the multiband broadband klystron under consideration. Early study of the possibility of employing the C-band Twystron output circuit in the interspersed arrangement in order to achieve the wide bandwidth capability of the amplifier were discouraging because of the length of the TWT circuit and the necessity for a short sever spacing, the distance between the previous klystron input circuit cavity and the beginning of the Twystron TWT output circuit.

The VA-913, then, would be an excellent candidate for C-band coverage in the suggested two-tube radar, needing only the addition of a gridded electron gun in place of the present cathode-pulsed electron gun. At S-band a number of choices exist, but a VA-145 type Twystron amplifier would probably be the best selection. A number of these devices are manufactured in small production quantities today. While capable of wide bandwidths, frequency coverage in each case has generally been limited to about 6% in response to customer requirements. Ten percent should certainly be attainable at S-band. Again, the new S-band device would require a gridded electron gun.

Use of two separate devices, as described, would seem to require the use of gridded guns in the devices for ease in pulse power input switching. Possibly

this may be viewed as objectionable from the point of view of device reliability. Alternately, mod-anode electron gun structures might be practicable, though the operating pulse width (10 μsec) is rather short for this type design. Mod-anode electron guns are ordinarily used in linear beam tubes operating at substantially longer pulse widths, i.e., ~100 μsec, where slow rise and fall times occasioned by modulator capacitance are not of particular concern. To the disadvantage of the electron gun grid or mod-anode requirement may be added the need for an additional electromagnet and power supplies, additional heater supply, additional power consumed, and ultimate logistic problems in field use when two different devices must be stocked.

The multiband broadband klystron approach may employ any electron gun configuration desired. Probably the simplest and most reliable design would make use of common cathode pulsing. In ultimate field use, a single device would be stocked, as opposed to two needed in the previous case. In small to moderate quantities, that is in lots of two to about thirty, the cost of the new device is not likely to be less than the cost of separate pairs of S-band and C-band tubes in the same quantities.

With regard to specific recommendations, the following is offered:

1. If the primary goal is to realize maximum technical capability in the radar, the two tube radar design should be explored. Existing broadband devices and/or modifications of them should be considered.

2. If the main goal concerns device logistics and simplicity in radar design, still with a reasonably high level of technical capability in the operational radar, then the multiband broadband klystron design should proceed apace.

MISSION
of
Rome Air Development Center

RADC plans and executes research, development, test and selected acquisition programs in support of Command, Control Communications and Intelligence (C^3I) activities. Technical and engineering support within areas of technical competence is provided to ESD Program Offices (POs) and other ESD elements. The principal technical mission areas are communications, electromagnetic guidance and control, surveillance of ground and aerospace objects, intelligence data collection and handling, information system technology, ionospheric propagation, solid state sciences, microwave physics and electronic reliability, maintainability and compatibility.